

Geochemical fingerprints and hydrocarbon potential of Paleocene mudrocks in the Tano Basin, Ghana: insights from biomarkers and stable carbon isotopes

Kojo Amoako¹  · Nancy Pearl Osei-Boakye² · Ningning Zhong² · N'Guessan Francois De Sales Konan² · Gordon Foli³ · Prince Opoku Appau⁴ · Clifford Fenyi⁵ · Ebenezer Apesegah⁵

Received: 16 August 2023 / Revised: 12 October 2023 / Accepted: 28 October 2023 / Published online: 17 November 2023

© The Author(s), under exclusive licence to Science Press and Institute of Geochemistry, CAS and Springer-Verlag GmbH Germany, part of Springer Nature 2023

Abstract The Paleocene mudrocks in Ghana's Tano Basin have received limited attention despite ongoing efforts to explore hydrocarbon resources. A thorough geochemical analysis is imperative to assess these mudrocks' petroleum generation potential and formulate effective exploration strategies. In this study, a comprehensive geochemical analysis was carried out on ten Paleocene rock cuttings extracted from TP-1, a discovery well within the Tano Basin. Various analytical techniques, including total organic carbon (TOC) analysis, Rock-Eval pyrolysis, gas chromatography-mass spectrometry, and isotope ratio-mass spectrometry, were employed to elucidate their hydrocarbon potential and organic facies. The findings in this study were subsequently compared to existing geochemical data on Paleocene source rocks in the South Atlantic marginal basins. The results indicated that the Paleocene samples

have TOC content ranging from 0.68 to 2.93 wt%. The prevalent kerogen types identified in these samples were Type II and Type III. Molecular and isotope data suggest that the organic matter found in the Paleocene mudrocks can be traced back to land plants and lower aquatic organisms. These mudrocks were deposited in a transitional environment with fluctuating water salinity, characterized by sub-oxic redox conditions. Maturity indices, both bulk and molecular, indicated a spectrum of maturity levels within the Paleocene mudrocks, spanning from immature to marginally mature, with increasing maturity observed with greater depth. In comparison, the organic composition and depositional environments of Paleocene source rocks in the Tano Basin closely resemble those found in the Niger Delta Basin, Douala, and Kribi-Campo Basins, the Kwanza Formation in Angola, and certain Brazilian marginal basins. However, it is worth noting that Paleocene source rocks in some of the basins, such as the Niger Delta and Brazilian marginal basins, exhibit relatively higher thermal maturity levels compared to those observed in the current Paleocene samples from the Tano Basin. In conclusion, the comprehensive geochemical analysis of Paleocene mudrocks within Ghana's Tano Basin has unveiled their marginal hydrocarbon generation potential. The shared geochemical characteristics between the Paleocene mudrocks in the Tano Basin and those in the nearby South Atlantic marginal basins offer valuable insights into source rock quality, which is crucial for shaping future strategies in petroleum exploration in this region.

✉ Kojo Amoako
kojamoako73@gmail.com

¹ Research Group for Marine Geochemistry (ICBM-MPI Bridging Group), Institute for Chemistry and Biology of the Marine Environment (ICBM), Carl von Ossietzky University Oldenburg, Ammerländer Heerstr., 26129 Oldenburg, Germany

² State Key Laboratory of Petroleum Resources and Prospecting, College of Geosciences, China University of Petroleum, Beijing 102249, China

³ Department of Geological Engineering, Faculty of Civil and Geo-Engineering, Kwame Nkrumah University of Science and Technology, Kumasi, Ghana

⁴ Ghana National Gas Company, 225 Osibisa Close, Airport West, Accra, Ghana

⁵ Petroleum Corporation, GNPC, PMB, Petroleum House, Tema, Ghana

Keywords Paleocene source rocks · Source input · Depositional environment · Thermal maturity · Hydrocarbon potential · Tano Basin · West Africa

1 Introduction

The Tano Basin (Fig. 1a), situated along the West African coastal margin, holds significant promise for hydrocarbon exploration (Kesse 1985; Brownfield and Charpentier 2006). This region has yielded three substantial petroleum fields: TEN, Jubilee, and Sankofa-Gye-Nyame. The success of these fields can be attributed to the presence of effective Cenomanian-Albian source rocks and turbidite sandstone reservoirs (Brownfield and Charpentier 2006; Atta-Peters and Garry 2014; Garry et al. 2016). Furthermore, the tectonic evolution of the basin has led to the formation of structural and stratigraphic traps characterized by shorter migration pathways for petroleum accumulation (Kelly and Doust 2016; Brownfield and Charpentier 2006). The seals in the Tano Basin, including the Albian shale series, Cenomanian shale series, Turonian shale series, and marine shale, exhibit high integrity and prevent the further migration of hydrocarbons beyond the reservoir rocks (Brownfield and Charpentier 2006). Presently, the cumulative daily crude oil production from the Jubilee and TEN Fields in the Tano Basin of Ghana amounts to roughly 230,000 barrels per day (bpd), with Jubilee contributing

around 180,000 bpd and TEN adding about 50,000 bpd (Panford 2022).

Recent studies have focused on the bulk geochemical composition, biomarkers, and isotopic characteristics of the Cretaceous source strata in the Tano Basin (Atta-Peters and Garry 2014; Garry et al. 2016; Bempong et al. 2019; Akaba et al. 2022; Abubakar et al. 2022; and Amoako et al. 2023). While preliminary studies have confirmed the commercial viability of the Cretaceous source strata for hydrocarbon generation, the Paleocene source rocks in this basin remain underexplored. The initial investigation by Atta-Peters and Salami (2004) aimed to delineate the marine depositional environment of the Paleocene source strata within the Tano Basin. Their research relied on dinoflagellate cyst assemblage analysis in Paleocene sediments extracted from the L 1S-3AX exploration well located offshore in the Tano Basin. Although paleontological datasets traditionally provide insights into sedimentary history and fossil records, biomarker and stable carbon isotope datasets offer enhanced sensitivity to alterations in the depositional environment. The high sensitivity of biomarker and isotope data is attributed to their organic matter origin, which is more responsive to environmental changes compared to the hard parts of fossils (Ogbesejana et al. 2023). Additionally,

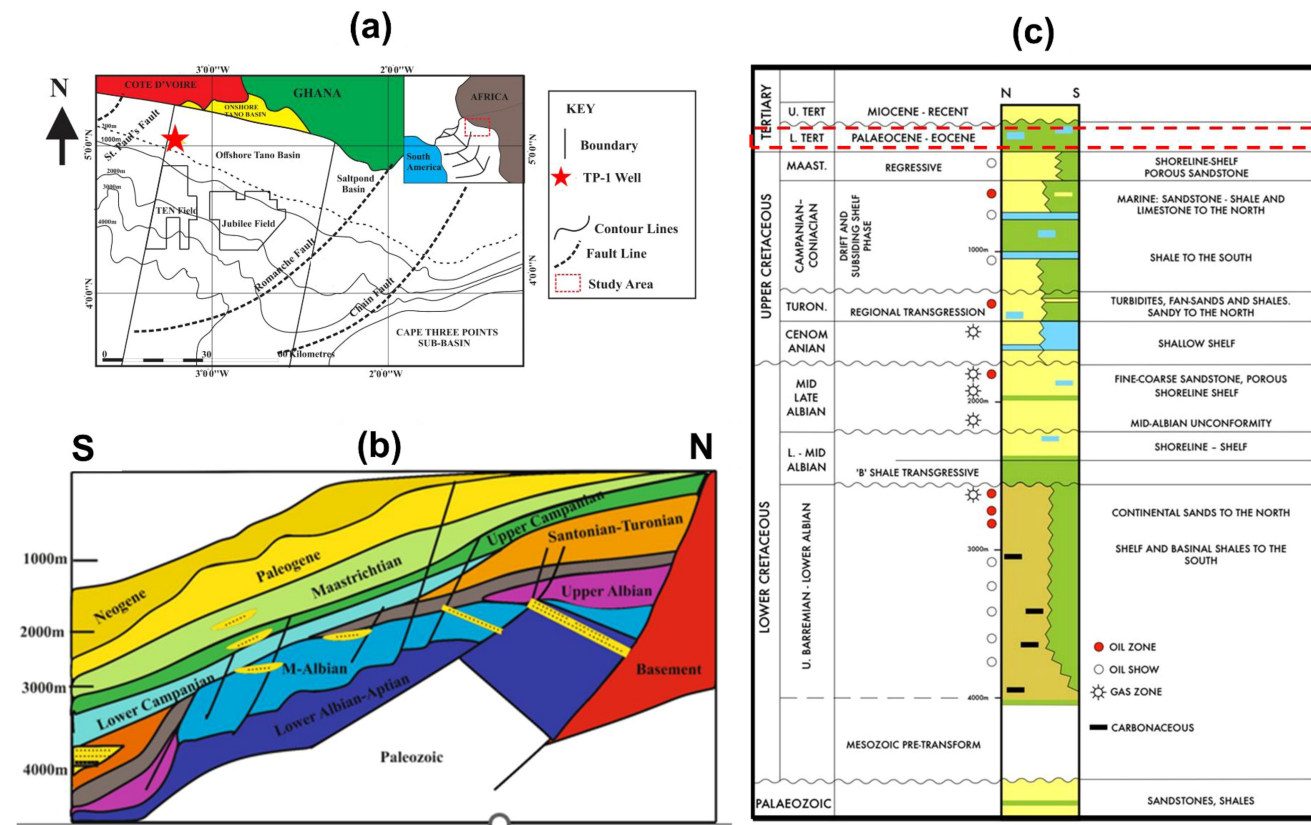


Fig. 1 **a** Geographical location of the Tano Basin showing the study well (TP-1) (GNPC, 2019) **b** Structural architecture of the Tano Basin (After Kelly and Doust 2016) **c** Generalized stratigraphy of the Tano Basin showing the studied stratum (Paleocene) (After Clontarf Energy Plc)

biomarkers and isotope data provide more precise information regarding the depositional setting (Bilal et al. 2023a, b). For instance, biomarkers facilitate the determination of redox conditions in the depositional environment, providing insights into the availability of oxygen and other electron acceptors (Didyk et al. 1978; Ten Haven et al. 1987). Furthermore, these data sources enable the identification of the source of organic matter in sediments, shedding light on depositional settings (Huang and Meinschein 1979; Volkman 1986; Liu et al. 2017; Amoako et al. 2023).

Currently, there is a lack of direct information available regarding the biomarkers or isotopic composition of Paleocene source rocks in the Tano Basin. As a result, there exists a significant gap in our knowledge concerning the origin and hydrocarbon potential of these potential source rocks in the Tano Basin. To address this knowledge gap, the study centers around a central research question: What is the organic composition and hydrocarbon generation potential of the Paleocene source rocks within the Tano Basin? The objectives include conducting a comprehensive assessment of these source rocks, encompassing organic richness, thermal maturity levels, biological sources of organic matter, and depositional settings through biomarker and stable carbon isotope analysis. The principal aim is to determine their hydrocarbon generation potential.

With increasing domestic demand for oil and gas, this research is crucial for enhancing our knowledge of the petroleum system and organic chemistry in the Tano Basin and similar basins along the South Atlantic margin. Many of the basins in these areas have similar geological histories (Schiefelbein et al. 2000; Beglinger et al. 2012a, b). The research, therefore, has the potential not only to enhance comprehension of the Paleocene source rock quality in the Tano Basin but also have a broader regional and global implications.

2 Study area

2.1 Regional and tectonic setting

The Tano Basin, shown in Fig. 1a, is a significant oil and gas production hub located in southeastern Ghana within West Africa's Gulf of Guinea (Bempong et al. 2019; Akaba et al. 2022). This basin is a crucial part of the extensive West African Transform Margin, which stretches from Senegal to Cameroon and includes other significant basins like the Niger Delta Basin and the Benue Trough (Brownfield and Charpentier 2006). Geographically, the Tano Basin is flanked by the St. Paul Fracture Zone in the northwest and the Romanche Fracture Zone in the southeast, both of which have significantly shaped its structural

development (Lake et al. 2014). The Tano Basin has a complex geological history, spanning epochs of significant tectonic activity. It commenced its tectonic evolution during the late Jurassic period, characterized by continental-to-oceanic rift processes (Lake et al. 2014). Over the course of its history, the basin has traversed a sequence of tectonically driven stages, encompassing continental rifting, oceanic expansion, and subsequent episodes of inversion and compression (Brownfield and Charpentier 2006).

2.2 Generalized stratigraphy of the Tano Basin

In this context, the lithology of each stratigraphic unit has been summarized using unpublished technical reports sourced from the Ghana National Petroleum Corporation. The stratigraphy of the Tano Basin encompasses various sedimentary rock types, including sandstones, shales, and limestones. These rocks were deposited at different stages in their tectonic history. In the Tano Basin, sedimentary deposits primarily range from the Eocene to the Aptian periods, with some Permian-age sediments encountered along the margin of the basin. These layers overlay Paleozoic basement rocks that are integral to an extensional rift basin system, as depicted in Fig. 1b.

2.2.1 Basement rocks (pre-cambrian)

The most ancient rocks underlying the Tano Basin comprise metamorphosed Precambrian Birimian igneous rocks, featuring schist, phyllite, and greywackes (Eisenlohr and Hirdes 1992). These rocks served as the foundation on which subsequent sedimentary layers were deposited.

2.2.2 Cenozoic era

The youngest of the Tano Basin's sedimentary fill corresponds to the Cenozoic Era, a geological epoch from approximately 66 million years ago to the present day. This era encompasses the following stratigraphic units:

2.2.2.1 Paleocene to eocene The lowest strata consist of both marine and non-marine sediments, comprising sandstones, siltstones, and shales. These rock strata often feature intervals rich in organic matter, making them potential source rocks for hydrocarbon reservoirs.

2.2.2.2 Miocene to Pliocene Overlying the older sedimentary layers are deposits from the Miocene and Pliocene epochs, comprising sands, clays, and conglomerates. These formations may contain reservoirs that house accumulations of oil and natural gas.

2.2.3 Cretaceous era

Beneath the Cenozoic sedimentary layers, there are rocks from the Cretaceous period, dating back to approximately 145–66 million years ago. These layers include formations known as the Cenomanian–Turonian and the Coniacian–Santonian series, notable for their marine shale and sandstone units.

2.2.4 Jurassic and triassic eras

At greater depths within the basin, sedimentary strata from the Jurassic and Triassic Eras become evident. These rock layers consist of sandstones, shales, and limestones and have the potential to serve as reservoirs or source rocks, depending on their unique compositions and organic content.

2.2.5 Permian and more ancient strata

In specific areas along the margins of the Tano Basin, older sedimentary formations from the Permian period and even more ancient geological epochs become apparent. These formations consist of various sediment types, including sandstones, shales, and limestone. Their potential for containing hydrocarbons depends on their distinct attributes and characteristics.

3 Materials and methods

3.1 Samples

The scientific investigation entailed a comprehensive geochemical analysis of ten Paleocene Mudrock samples acquired from the TP-1 well, an exploration well located in the Tano Basin (Fig. 1a). Additional information regarding the stratigraphy of the Tano Basin, the specific type of Paleocene samples analyzed, and the depths at which sampling occurred can be found in Table 1. The representative samples were selected based on gamma log data. All experimental procedures were conducted at the State Key Laboratory for Petroleum Resources and Prospecting situated in Beijing.

3.2 Total organic carbon (TOC) and rock pyrolysis experiment

Following the guidelines provided by Jarvie (1991), the Leco CS230 analyzer was utilized for conducting total organic carbon (TOC) analysis. Furthermore, the pyrolysis experiment adhered to the standard procedures outlined in GB/T 18602-2001 and was performed using the Rock-Eval

machine, OGE-IV. These tests were conducted in the preliminary screening stage to assess the quantity, quality, and maturity of organic materials present. For data interpretation, templates and guidelines created by Peters and Cassa (1994), Espitalie et al. (1977), and Carvajal-Ortiz and Gentzis (2015) were referred to.

3.3 Extraction and separation process

Extractable organic matter (EOM) was extracted from a batch of ten Paleocene samples, totaling approximately 100 g of finely ground rock-cutting samples. A solvent mixture of 400 mL dichloromethane and methanol (in a ratio of 93.7 %) was employed for reflux extraction, lasting 48 h, to extract hydrocarbons. Subsequently, the resulting mixture was dissolved in 50 mL of petroleum ether and filtered through a cotton-stuffed funnel to eliminate insoluble compounds, specifically asphaltenes. The filtered solution was then subjected to fractionation, separating it into saturated hydrocarbons, aromatic hydrocarbons, and resin using a standard column packed with silica gel and alumina. The fractionation process involved the sequential addition of petroleum ether, a mixture of dichloromethane and petroleum ether (in a ratio of 2:1%), and a mixture of dichloromethane and methanol (in a ratio of 93.7%) to the column.

3.4 Molecular analysis

An Agilent 6890 gas chromatograph (GC) equipped with an HP-5 MS fused silica capillary column and linked to an Agilent Model 5975i mass selective detector was employed to analyze saturated molecular markers in the rock extracts. The GC–MS system's configuration involved initiating the oven temperature at 50 °C for 1 min, followed by a sequential increase to 120 °C at a rate of 20 °C/min, and then to 310 °C at a rate of 3 °C/min over 10 min.

For the evaluation of aromatic hydrocarbon fractions, the Agilent 5975i GC–MS system was also utilized, featuring an HP-5 MS fused silica capillary column (60 m × 0.25 mm i.d., 0.25 µm film thickness) composed of 5% phenyl-methylpolysiloxane. In this case, the GC conditions commenced with an initial temperature of 80 °C for 1 min, followed by a gradual increase to 310 °C at a rate of 3 °C/min, maintained for 16 min, while keeping the injector temperature at 300 °C.

In all the techniques above, helium served as the carrier gas, and the mass spectrometer operated in electron impact (EI) mode with an ionization energy of 70 eV and a scan range of 50–600 Da. The retention times of the samples' saturated and aromatic molecular markers were compared to those of a thoroughly defined reference sample used as the standard for this study in the interest of identification.

Table 1 Bulk geochemical parameters used to assess the organic richness, abundance, and maturity of organic matter in Paleocene mudrock samples from the TP-1 well, located in the Tano Basin

Sample ID	Strata	Well	Depth (m)	Sample Type	Lithology (wt%)	TOC	S1 (mg HC/grock)	S2 (mg HC/grock)	S3 (mg HC/grock)	GP(S1 + S2) (mg HC/grock)	P1 (S1/(S1 + S2))	HI (S2/TOC)*100 mg (HC/g TOC)	Tmax (°C)
T1	Paleocene	TP-1	975	Cuttings	Claystone	0.68	0.63	0.69	1.28	0.54	1.32	0.48	101.86
T2	Paleocene	TP-1	1050	Cuttings	Claystone	0.75	0.43	0.75	1.29	0.58	1.17	0.35	100.02
T3	Paleocene	TP-1	1113	Cuttings	Claystone	0.81	0.22	0.80	1.29	0.62	1.02	0.22	98.18
T4	Paleocene	TP-1	1190	Cuttings	Claystone	1.59	0.35	3.06	1.42	2.03	3.40	0.15	161.45
T5	Paleocene	TP-1	1250	Cuttings	Claystone	2.36	0.47	5.31	1.54	3.45	5.78	0.08	224.71
T6	Paleocene	TP-1	1300	Cuttings	Claystone	2.54	0.58	5.16	1.49	3.46	5.73	0.10	204.54
T7	Paleocene	TP-1	1341	Cuttings	Claystone	2.71	0.68	5.00	1.44	3.47	5.68	0.12	184.37
T8	Paleocene	TP-1	1433	Cuttings	Claystone	2.93	0.85	5.53	1.45	3.81	6.38	0.13	189.06
T9	Paleocene	TP-1	1460	Cuttings	Claystone	2.90	0.79	6.17	1.38	4.47	6.96	0.11	212.91
T10	Paleocene	TP-1	1497	Cuttings	Claystone	2.84	1.12	6.14	1.44	4.26	7.26	0.15	215.89

where *TOC* total organic carbon, *GP* genetic potential, *P1* production index, *HI* hydrogen index

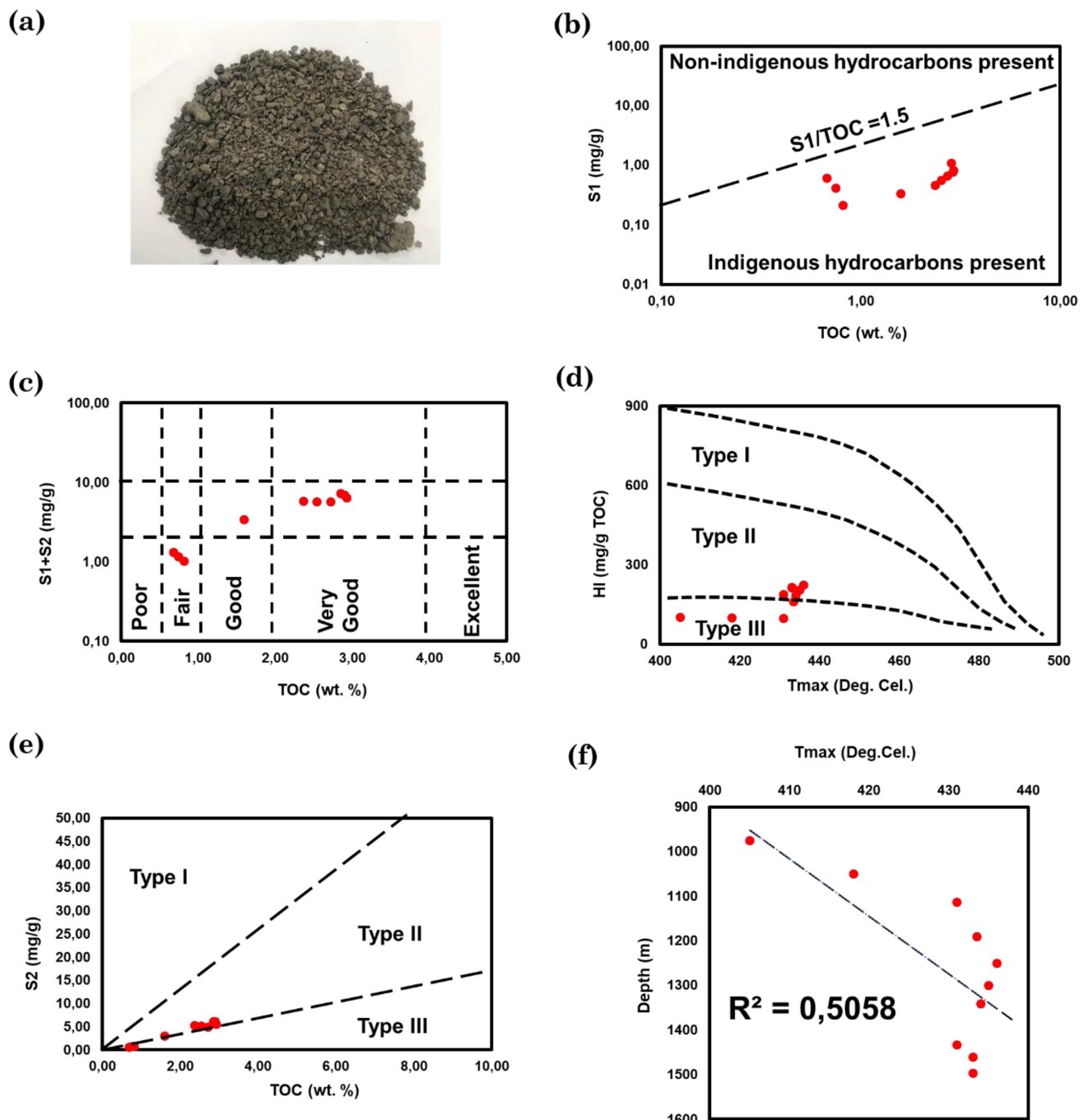


Fig. 2 **a** Representative sample of Paleocene sediments from the Tano Basin **b** Plot of S_1 (free hydrocarbons from rock pyrolysis) and total organic carbon (TOC) content showing indigenous and non-indigenous hydrocarbons (After Hunt 1966) **c** Variation of genetic potential ($S_1 + S_2$) versus TOC showing the organic richness **d** Plot of hydrogen index versus T_{max} showing kerogen types **e** Plot of S_2 and TOC showing kerogen types **f** Plot of T_{max} versus depth showing the bulk maturity profile of organic matter in Paleocene mudrock samples from TP-1 well, Tano Basin

3.5 Stable carbon isotope ratio analysis

The asphaltene isolates were analyzed using an elemental analyzer–isotope ratio mass spectrometer (EA–IRMS). Approximately 0.3 mg of each asphaltene sample and the analytical standard were accurately placed into small tin

sample cups for isotope analysis. Subsequently, a zero-blank autosampler was employed to introduce the samples into a Dumas combustion EA, where they underwent combustion at a temperature of 1030 °C with oxygen present. The resulting combustion products were directed into a preparative gas chromatography (GC) column using

Table 2 Selected n-alkane and hopanoid parameters for assessing the depositional environment of organic matter in Paleocene mudrock samples from TP-1 Well, Tano Basin

Sample ID	Strata	Well	Depth	Sample Type	Lithology	Pr/Ph	Ph/nC ₁₈	Pr/nC ₁₇	GI	C ₂₉ H/C ₃₀ H	C ₃₀ D/C ₂₉ Ts
T1	Paleocene	TP-1	975	Cuttings	Claystone	1.43	1.79	3.29	0.28	0.74	0.14
T2	Paleocene	TP-1	1050	Cuttings	Claystone	1.48	2.05	3.46	0.25	0.63	0.19
T3	Paleocene	TP-1	1113	Cuttings	Claystone	1.46	2.18	3.96	0.23	0.80	0.16
T4	Paleocene	TP-1	1190	Cuttings	Claystone	1.53	2.31	3.63	0.21	0.53	0.23
T5	Paleocene	TP-1	1250	Cuttings	Claystone	1.48	2.31	4.04	0.25	0.75	0.25
T6	Paleocene	TP-1	1300	Cuttings	Claystone	1.48	2.31	4.04	0.20	0.61	0.22
T7	Paleocene	TP-1	1341	Cuttings	Claystone	1.44	2.30	4.45	0.15	0.83	0.19
T8	Paleocene	TP-1	1433	Cuttings	Claystone	1.37	2.25	3.61	0.19	0.64	0.17
T9	Paleocene	TP-1	1460	Cuttings	Claystone	1.39	2.13	3.11	0.16	0.63	0.15
T10	Paleocene	TP-1	1497	Cuttings	Claystone	1.30	2.20	2.77	0.08	0.63	0.11

Fig. 3 Gas chromatograms of saturated hydrocarbon fractions in Paleocene mudrock samples from TP-1 well, Tano Basin

a Representative saturated fraction mass chromatograms (m/z 85) showing nC_{15} – nC_{33} n-alkane fraction and isoprenoids, Pristane (Pr), Phytane (Ph), n -heptadecane (Pr/ nC_{17}) and n -octadecane (Ph/ nC_{18}) distribution **b** Representative saturated fraction mass chromatograms (m/z 191) showing C₁₉TT–C₂₉TT: tricyclic terpanes with different carbon numbers; C₂₄E: tetracyclic terpane, C₂₉H: C₂₉ hopane; C₃₀H: C₃₀ hopane; Ts: C₂₇18 α (H)-22,29,30-trinorhopane; Tm: C₂₇17 α (H)-22,29,30-trinorhopane and C₃₁–C₃₂ homohopanes (HH) and **c** Representative saturated fraction mass chromatograms (m/z 191) showing pregnanes (p), homopregnanes (hp), diasteranes (DSt), regular steranes (St) and methyl steranes (Me) hydrocarbons

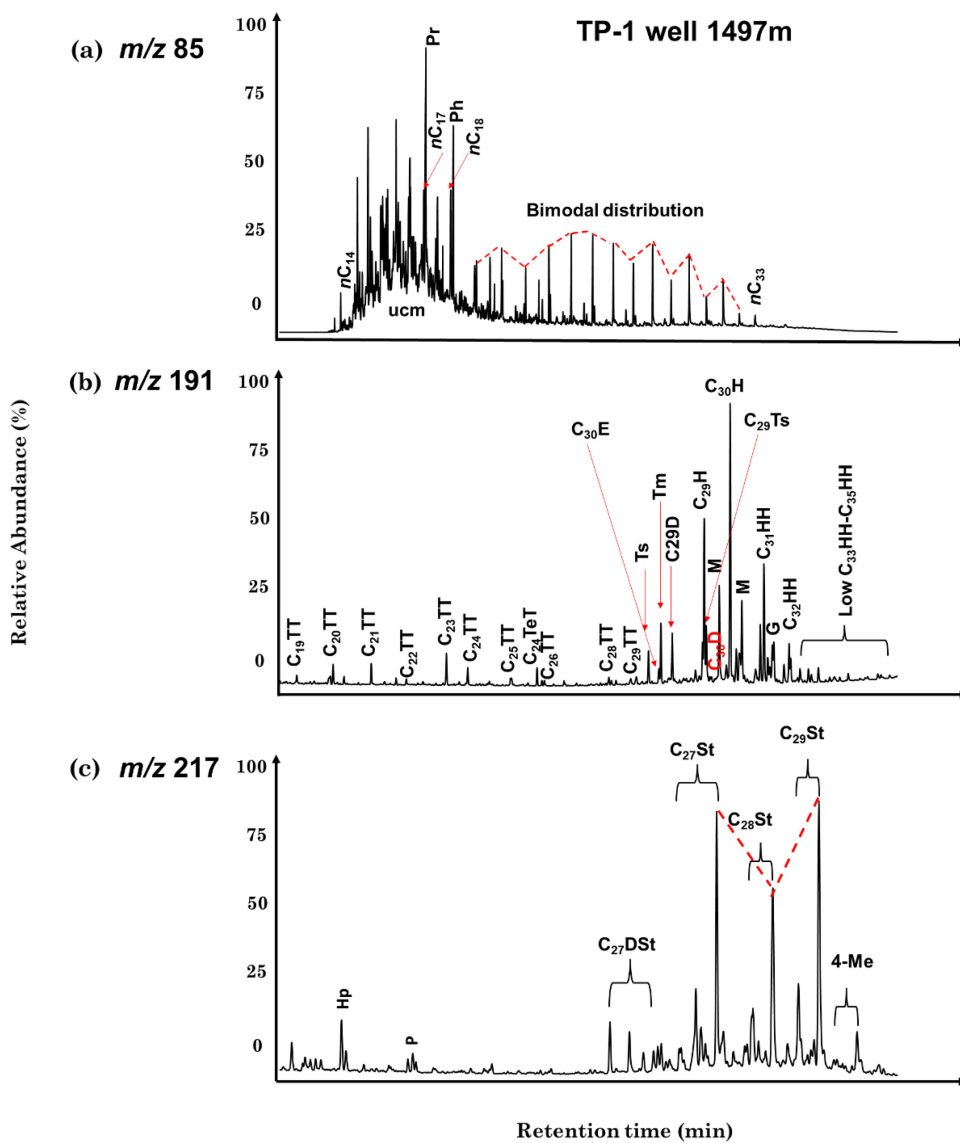


Table 3 Aliphatic and aromatic molecular parameters for assessing the organic matter maturity in Paleocene mudrock samples from TP-1 Well, Tano Basin

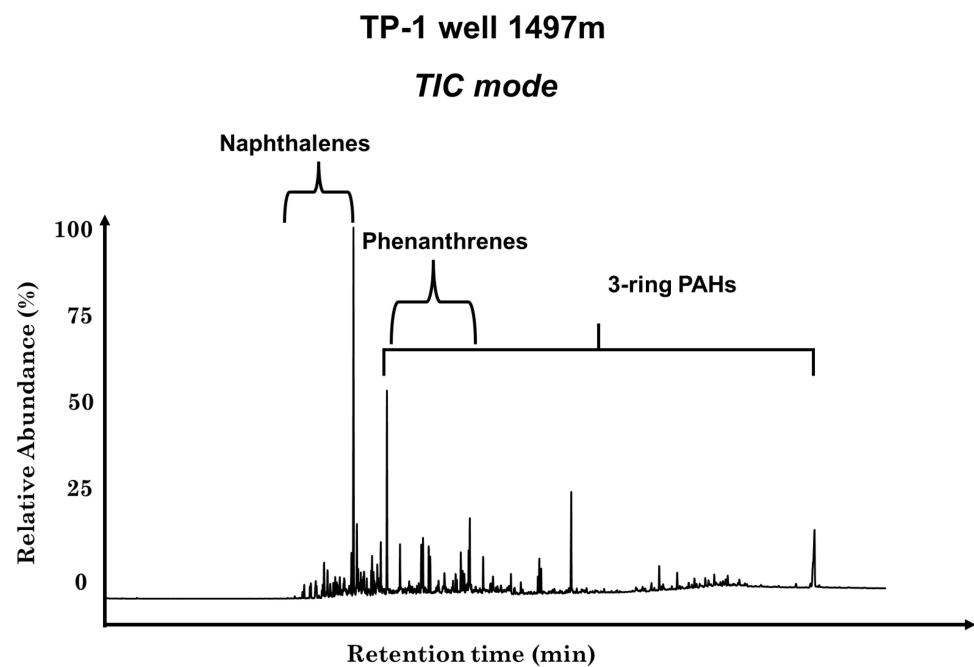
Sample ID	Strata	Well	Depth (m)	Sample Type	Lithology	Ts/ (Ts + Tm)	C ₃₁ H _{22S/} (22S + 22R)	C ₂₀ S/ (20S + 20R)	MPI- 1	MPI- 2	MPI- 3	MDR	MNR- 1	TNR- 1	Rc (%)	
T1	Paleocene	TP- 1	975	Cuttings	Claystone	0.22	0.22	0.29	0.56	0.66	1.26	1.53	2.65	1.64	1.21	0.75
T2	Paleocene	TP- 1	1050	Cuttings	Claystone	0.28	0.31	0.30	0.46	0.56	1.11	1.33	2.32	1.38	1.01	0.65
T3	Paleocene	TP- 1	1113	Cuttings	Claystone	0.34	0.31	0.31	0.56	0.65	1.16	1.33	2.18	1.31	1.01	0.75
T4	Paleocene	TP- 1	1190	Cuttings	Claystone	0.28	0.28	0.30	0.53	0.62	1.18	1.40	2.38	1.44	1.08	0.72
T5	Paleocene	TP- 1	1250	Cuttings	Claystone	0.31	0.29	0.30	0.72	0.82	1.14	1.37	2.33	1.57	1.17	0.73
T6	Paleocene	TP- 1	1300	Cuttings	Claystone	0.31	0.29	0.29	0.81	0.91	1.13	1.36	2.30	1.64	1.22	0.73
T7	Paleocene	TP- 1	1341	Cuttings	Claystone	0.29	0.30	0.30	0.86	0.96	1.12	1.36	2.28	1.67	1.25	0.74
T8	Paleocene	TP- 1	1433	Cuttings	Claystone	0.31	0.29	0.28	0.91	1.01	1.11	1.35	2.27	1.70	1.27	0.74
T9	Paleocene	TP- 1	1460	Cuttings	Claystone	0.35	0.27	0.26	0.93	1.02	1.08	1.32	1.97	1.60	1.22	0.75
T10	Paleocene	TP- 1	1497	Cuttings	Claystone	0.39	0.31	0.30	0.95	1.03	1.05	1.29	1.66	1.49	1.16	0.76

Table 4 Selected *n*-alkane parameter and distribution of regular steranes (St) and diasteranes (DSt) for identifying organic matter sources and depositional environment in Paleocene mudrock samples from TP-1 Well, Tano Basin

Sample ID	Strata	Well	Depth	Sample type	Lithology	$(nC_{21} + nC_{22})/(nC_{28} + nC_{29})$	% C ₂₇ St	% C ₂₈ St	% C ₂₉ St	C ₂₇ St/ C ₂₉ St	C ₂₇ DSt/ C ₂₇ St
T1	Paleocene	TP-1	975	Cuttings	Claystone	0.90	30.32	26.64	43.04	0.70	0.15
T2	Paleocene	TP-1	1050	Cuttings	Claystone	1.05	29.85	29.06	41.09	0.73	0.25
T3	Paleocene	TP-1	1113	Cuttings	Claystone	1.02	29.38	31.49	39.13	0.75	0.34
T4	Paleocene	TP-1	1190	Cuttings	Claystone	0.97	30.01	28.32	41.67	0.72	0.22
T5	Paleocene	TP-1	1250	Cuttings	Claystone	0.89	29.70	30.00	40.29	0.74	0.28
T6	Paleocene	TP-1	1300	Cuttings	Claystone	1.08	30.03	28.52	41.45	0.73	0.22
T7	Paleocene	TP-1	1341	Cuttings	Claystone	0.93	29.74	30.39	39.86	0.75	0.29
T8	Paleocene	TP-1	1433	Cuttings	Claystone	0.94	30.10	29.30	40.60	0.74	0.23
T9	Paleocene	TP-1	1460	Cuttings	Claystone	1.05	29.89	31.95	38.16	0.78	0.31
T10	Paleocene	TP-1	1497	Cuttings	Claystone	1.04	30.40	32.42	37.18	0.82	0.29

helium as the carrier gas and were subsequently dehydrated using a MgCl₂ trap. Carbon dioxide (CO₂) was effectively isolated via chromatography. To further measure carbon isotopes, the purified CO₂ was then injected into the

Micromass Optima IRMS through an open split. The reported carbon isotope values represent the average of multiple replicate analyses, typically exceeding two (n > 2), and exhibiting a standard deviation of less than

Fig. 4 Total ion current (TIC) chromatogram of the aromatic hydrocarbon showing the summed intensity of 2-ring and 3-ring polycyclic aromatic hydrocarbons identified in Paleocene mudrock samples from TP-1 well, Tano Basin

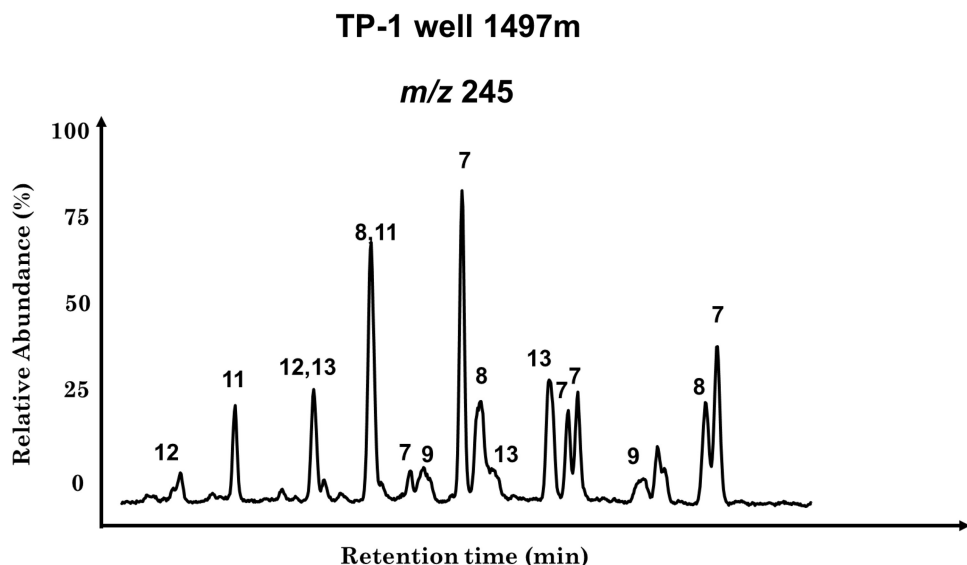


Fig. 5 Representative aromatic hydrocarbon fraction mass chromatograms (m/z 245) showing the distribution of methyl triaromatic steroids in Paleocene mudrock samples from TP-1 well, Tano Basin. Peak 7: 4,23,24-trimethyltriaromatic steroids (C_{29} triaromatic steroids), peak 8: 4-methyl-24-ethyltriaromatic steroids (C_{29} triaromatic steroids), peak 9: 3-methyl-24-ethyltriaromatic steroids (C_{29} triaromatic steroids), peak 11: 4-methyltriaromatic steroids (C_{27} triaromatic steroids), peak 12: 3-methyltriaromatic steroids (C_{27} triaromatic steroids), peak 13: 3,24-dimethyltriaromatic steroids (C_{28} triaromatic steroids)

0.2‰. These values are referenced to the widely recognized standard, Vienna Pee Dee Belemnite (VPDB) carbonate.

4 Results

4.1 TOC and rock pyrolysis

The lithology of the Paleocene source strata consists of medium to dark gray,

occasionally pale gray and brownish gray, moderately firm to hard, blocky to platy, and non-calcareous shale/claystone (Fig. 2a). This shale/claystone also contains minor fine-grained unconsolidated sandstones, siltstones, and limestone intercalations. In some regions, it is possible to encounter sporadic swelling streaks of disseminated pyrite, along with rare occurrences of pyrite modules.

The TOC values obtained from the Paleocene mudrocks range from 0.7 wt% to approximately 2.9 wt% (Fig. 2b and Table 1). Notably, there is a discernible increasing trend in these values as depth increases (Table 1). The rock pyrolysis parameters, specifically $S_1 + S_2$, which assess the hydrocarbon potential of petroleum samples, fall within the range of 1–7 mg HC/g rock (Fig. 1c). Hydrogen index (HI) values observed in the Paleocene samples vary from 98 to 215 mg HC/g (Table 1 and Fig. 1d). Tmax, representing the temperature at which the maximum rate of hydrocarbon generation occurs during pyrolysis analysis of

kerogen samples, ranges between 405 and 436 °C in the Paleocene samples (Fig. 2f). It is worth noting that HI, $S_1 + S_2$, and Tmax values all exhibit an increase with depth in the Paleocene source samples (Table 2 and Fig. 2b–f).

4.2 Molecular composition of the samples

4.2.1 Aliphatic hydrocarbons

In this section, a detailed saturated biomarker analysis is presented for the indigenous hydrocarbons identified in the Paleocene samples. The indigeneity of the hydrocarbons was established by plotting S_1 against TOC, as indicated in Fig. 2b. In all the samples, the S_1/TOC values in the Paleocene samples are below 1.5, indicating that the associated hydrocarbons are of indigenous origin (Fig. 2b; Hunt 1966).

Within the aliphatic fraction of the Paleocene extracts, there is a hump pattern between the lower-weight and intermediary-weight normal alkanes (Fig. 3a) suggesting that the Paleocene mudrocks may contain an unresolved Complex Mixture (UCM). The UCM hump could be attributed to contamination, biodegradation, or limitations of GC-MS in accurately detecting and separating hydrocarbons in the samples, as noted by Gough and Rowland (1990). However, pristane and phytane (Pr and Ph) seem to be preserved within the normal alkanes, showing a bimodal distribution pattern (Fig. 3a). The calculated Pr/Ph ratios fall within the range of 1.48–1.70, accompanied by notably

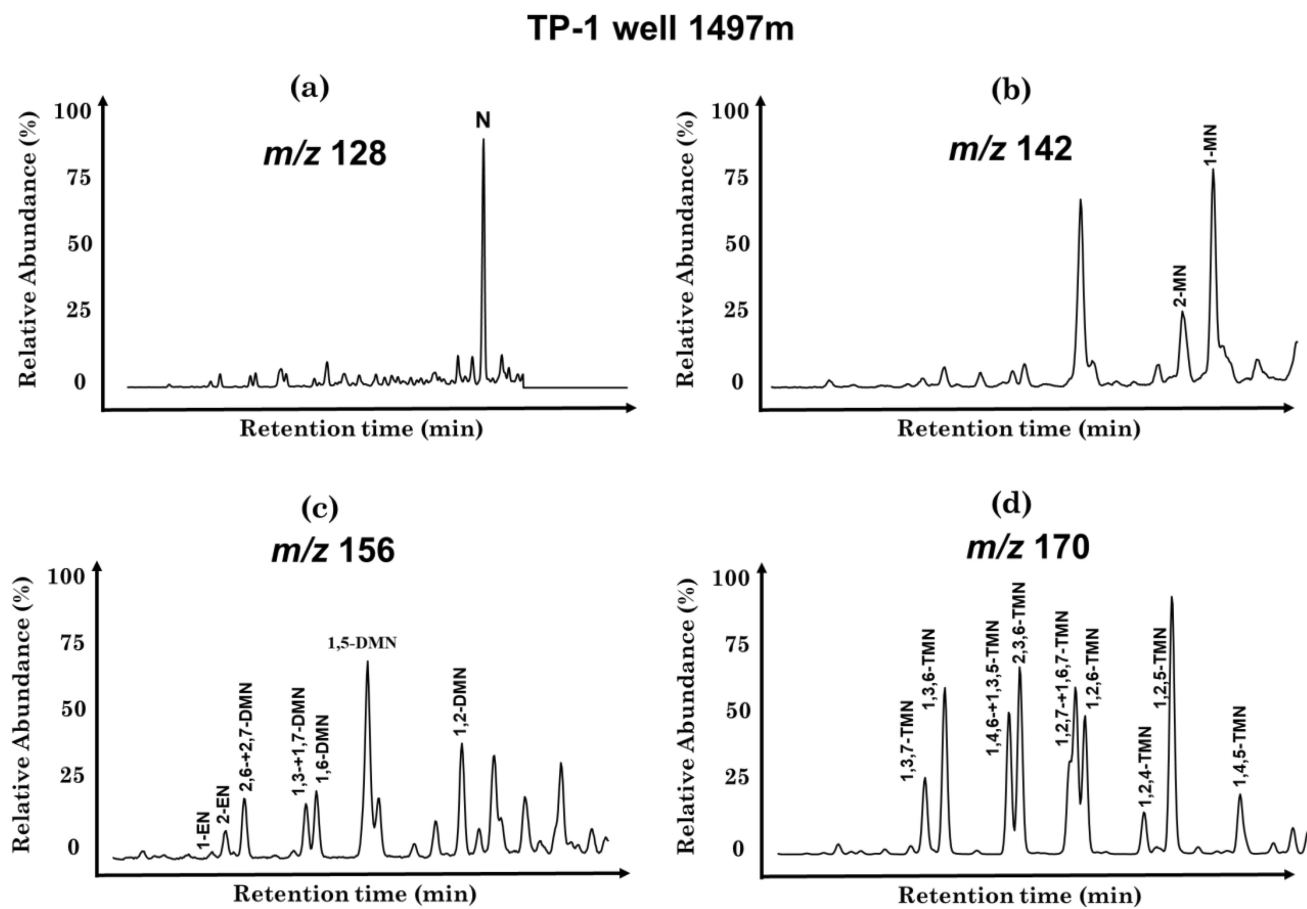


Fig. 6 **a** Representative aromatic hydrocarbon fraction mass chromatograms (m/z 128) showing naphthalene **b** Representative aromatic hydrocarbon fraction mass chromatograms (m/z 142) showing methyl naphthalene **c** Representative aromatic hydrocarbon fraction mass chromatograms (m/z 156) showing dimethyl naphthalene **d** Representative aromatic hydrocarbon fraction mass chromatograms (m/z 170) showing trimethyl naphthalene in Paleocene mudrock samples from TP-1 well, Tano Basin

elevated average ratios of isoprenoids to n -alkanes, specifically $\text{Pr}/n\text{-C}_{17}$ and $\text{Ph}/n\text{-C}_{18}$ (Table 2). The identification of specific compounds from the pentacyclic terpane group was achieved, including trisnorhopane (Ts), trimethylandrostane (Tm), C_{30} early eluting rearranged hopane (C_{30}E), C_{29} hopane, C_{30} hopane, C_{30} diahopane, gammacerane, and C_{31} extended hopanes in the Paleocene samples. Figure 3b provides a visual representation of this identification. Furthermore, as shown in Fig. 3b, the peak intensity of C_{32} – C_{35} homohopanes was low at m/z 191, but the abundance of C_{31} homohopane is noticeably high. Additionally, the tricyclic and tetracyclic terpanes (TT and TeT) homologs ranged from C_{19} to C_{29} , with the main C_{24} tetracyclic terpane and C_{23}TT being prominent.

The Paleocene samples exhibited greater C_{30} hopane peaks than C_{29} diahopane peaks, and the majority of them had substantial gammacerane peaks (Gammacerane/ C_{30} hopane > 0.2), with the samples' $\text{C}_{30}\text{D}/\text{C}_{29}\text{TS}$ ratios ranging from 0.11–0.25 (Table 2). The homohopane maturity metric $\text{C}_{31}22\text{S}/(22\text{S} + 22\text{R})$ ranged between 0.22

and 0.31, whereas the trisnorhopane thermal indicator $\text{Ts}/(\text{Ts} + \text{Tm})$ had average ratios between 0.22 and 0.39 (Table 3).

Regarding the steranes and diasteranes pattern, the C_{29} steranes were more prevalent than the C_{27} steranes, which were likewise more abundant than the C_{28} steranes in the Paleocene samples. Lower peak intensities of pregnanes and 4-methylcholestane (4-Me) were observed (Fig. 3c), and all the samples had lower average ratios of C_{27} Diasterane/ C_{27} regular Sterane (Table 4).

4.2.2 Aromatic hydrocarbons

In the Paleocene samples, analysis of the chromatograms in the total ion chromatogram (TIC) mode revealed the presence of various 2–3-ring aromatic hydrocarbons. These compounds include naphthalene, phenanthrenes, triaromatic steroids, fluorenes, dibenzothiophenes, and dibenzofurans (F, DBT, and DBF) (Fig. 4). The study indicates that the Paleocene samples exhibit relatively higher peaks

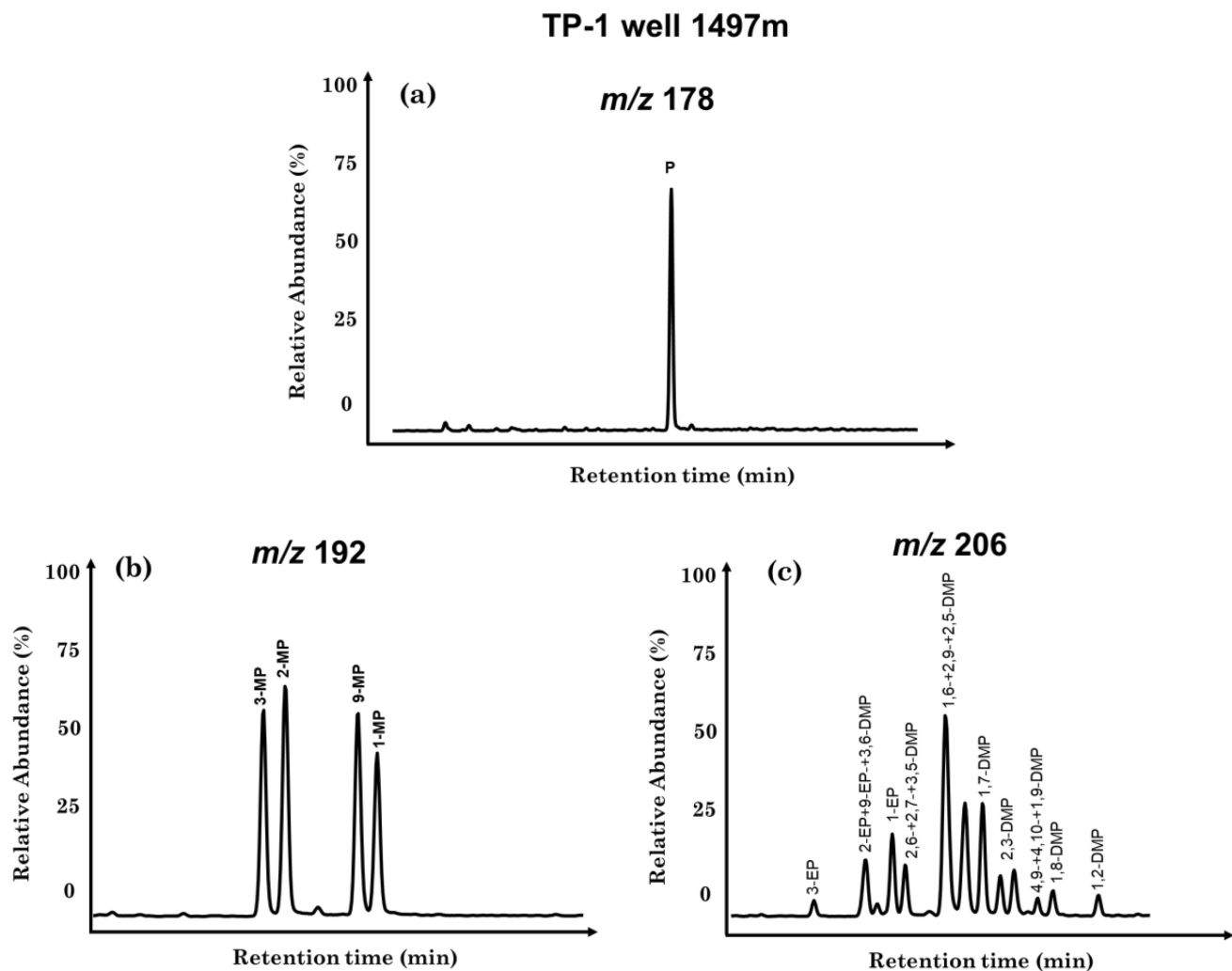


Fig. 7 **a** Representative aromatic hydrocarbon fraction mass chromatograms (m/z 178) showing Phenanthrene **b** Representative aromatic hydrocarbon fraction mass chromatograms (m/z 192) showing methyl phenanthrene **c** Representative aromatic hydrocarbon fraction mass chromatograms (m/z 206) showing dimethyl phenanthrene in Paleocene mudrock samples from TP-1 well, Tano Basin

of 2-ring polycyclic aromatic hydrocarbons (PAH) compared to 3-ring PAH, with naphthalene being particularly prominent. Various mass-to-charge ratios were utilized to distinguish and analyze the mass spectrum of the aromatic compounds and their isomers within the samples. This approach provided further insights into the distribution of aromatic compounds (Figs. 5, 6, 7, 8, 9 and 10).

Additionally, Table 5 and Fig. 12b illustrate the uneven distribution of heterocyclic aromatic compounds (HTCs) and hydrocarbons, such as DBT, DBF, and Fs, along with their alkyl derivatives, within the Paleocene samples. The relative abundance of these HTCs is ranked as DBF > DBT > F (Table 5).

Due to the challenges of measuring vitrinite reflectance on rock cuttings, alternative measures of the thermal maturity of organic matter were employed. Notably, ratios involving alkyl naphthalenes and alkyl phenanthrenes from

analogous studies were utilized (Radke et al. 1982, 1986; Yuzhuang et al. 2005; Asif et al. 2011; Amoako et al. 2023). Table 3 and Fig. 15 present the eight selected aromatic characteristics used to assess the maturity levels of Paleocene rock samples in the Tano Basin.

4.3 Stable carbon isotope analysis

The Paleocene samples stable carbon isotope ratios point to a heavier signal (Table 6). These samples' average $^{13}\text{C}_{\text{Sat}}$ values are $-27.88\text{\textperthousand}$, with a range of $-27.67\text{\textperthousand}$ to $-28.18\text{\textperthousand}$, and their average $^{13}\text{C}_{\text{Aro}}$ values are relatively heavier, varying between $-26.42\text{\textperthousand}$ and $-27.56\text{\textperthousand}$. The $\Delta\delta_{\text{Aro}}-\Delta\delta_{\text{Sat}}$ values in the studied Paleocene samples range between 0.1 and 1.55 (Table 6).

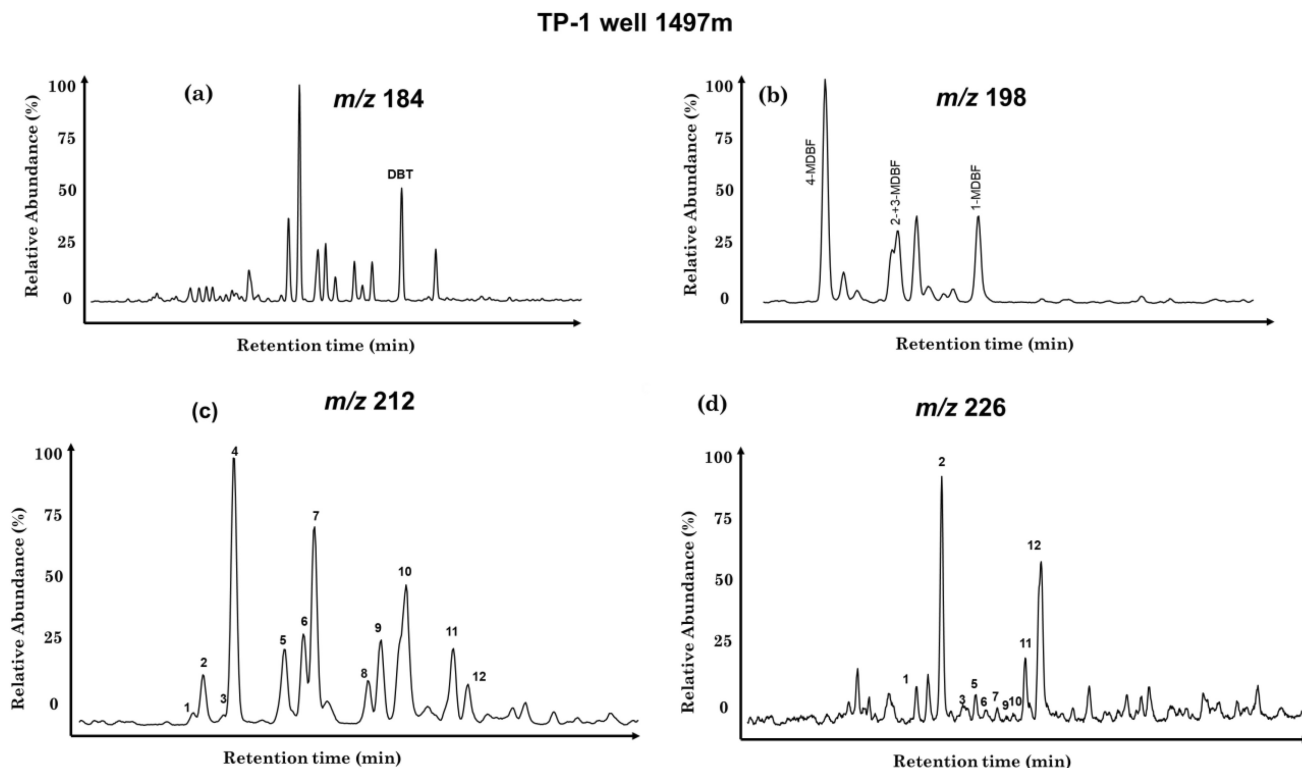


Fig. 8 **a** Representative aromatic hydrocarbon fraction mass chromatograms (m/z 184) showing dibenzothiophene **b** Representative aromatic hydrocarbon fraction mass chromatograms (m/z 198) showing methyl dibenzothiophene **c** Representative aromatic hydrocarbon fraction mass chromatograms (m/z 212) showing dimethyl dibenzothiophene **d** Representative aromatic hydrocarbon fraction mass chromatograms (m/z 226) showing trimethyl dibenzothiophene in Paleocene mudrock samples from TP-1 well, Tano Basin

5 Discussions

5.1 Source input analysis

In this section, the biological origins of the organic matter in the Paleocene samples were deduced using both kerogen and biomarker parameters. The assessment of the kerogen composition in the mudstones relied on rock pyrolysis parameters, with a particular emphasis on examining the relationships between HI versus Tmax and TOC versus S2 (amount of hydrocarbons generated from the thermal decomposition of organic matter within a rock sample). HI values serve as indicators of kerogen type, where Type I kerogen is associated with high values (> 600 mg HC/g), Type II kerogen is characterized by moderate values (ranging from 300 mg HC/g to 600 mg HC/g), and Type III kerogen is represented by lower values (falling within the range of 50 mg HC/g to 200 mg HC/g) (Peters and Cassa 1994; Espitalie et al. 1977). As illustrated in Fig. 2d–e, the analysis reveals the coexistence of both Type II and Type III kerogens within the Paleocene mudrocks of the Tano Basin. Type II kerogen is derived from a combination of zooplankton, phytoplankton, and bacterial remains deposited in a reducing environment (Cheng et al. 2019).

On the other hand, Type III kerogen typically originates from the decomposition of land plants deposited in a terrestrial environment (Vandenbroucke and Largeau 2007). Therefore, the coexistence of Type II and Type III kerogen indicates the mixed sources of organic matter in the Paleocene samples from the Tano Basin.

Additionally, the n -alkane ratio, $(nC_{21} + nC_{22})/(nC_{28} + nC_{29})$, is valuable for distinguishing between continental and marine sources of organic matter at the molecular level (Curiale and Bromley 1996). A higher prevalence of lower molecular weight hydrocarbons ($\leq nC_{22}$) suggests a greater contribution from marine sources, while a higher abundance of higher molecular weight hydrocarbons ($\geq nC_{28}$) indicates a greater contribution from terrestrial sources. A ratio close to one for $(nC_{21} + nC_{22})/(nC_{28} + nC_{29})$ suggests the presence of both land-based and aquatic sources of organic matter. From Table 4, the $(nC_{21} + nC_{22})/(nC_{28} + nC_{29})$ ratio is nearly equal to one, indicating the coexistence of lower marine aquatic organisms and higher plant precursors in the Paleocene samples. This finding aligns with the identified kerogen type, providing further support for the analysis.

Furthermore, the $Pr/n\text{-}C_{17}$ versus $Ph/n\text{-}C_{18}$ plot serves as a valuable tool for interpreting organic sources and

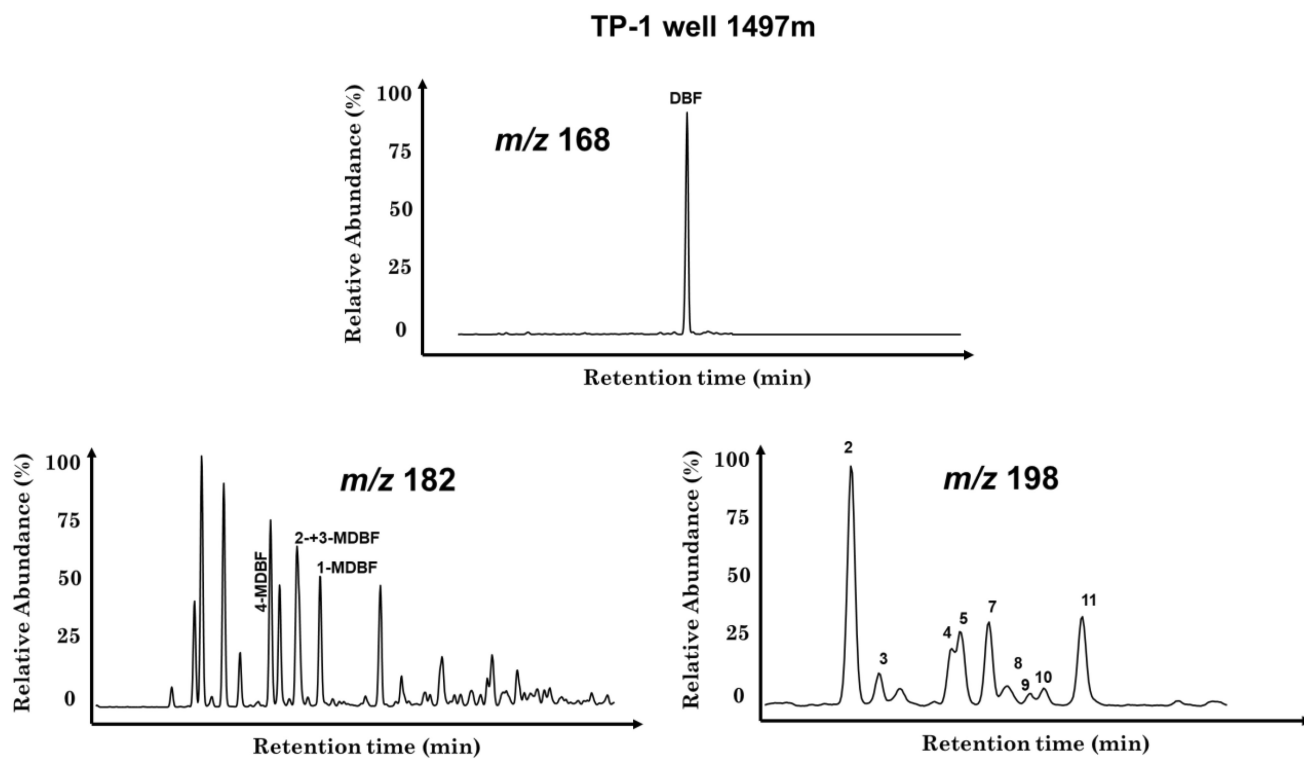


Fig. 9 **a** Representative aromatic hydrocarbon fraction mass chromatograms (m/z 168) showing dibenzofuran **b** Representative aromatic hydrocarbon fraction mass chromatograms (m/z 182) showing methyl dibenzofuran **c** Representative aromatic hydrocarbon fraction mass chromatograms (m/z 212) showing dimethyl dibenzofuran in Paleocene mudrock samples from TP-1 well, Tano Basin

paleoenvironmental conditions (Connan and Cassou 1980; Shanmugam 1985; Chen et al. 2018). According to this relationship, the results of this study indicate a predominance of mixed organic matter input (Fig. 11b).

Moreover, regular steranes are a type of biological marker commonly found in petroleum and hydrocarbon source rocks, originating from the sterols of cell membranes of eukaryotes, including algae and higher plants (Volkman 2005). The relative ratios of regular steranes C_{27} , C_{28} , and C_{29} can indicate the source of the organic matter. C_{27} regular steranes are typically associated with lower aquatic organisms, such as marine zooplankton and algae, while C_{29} regular steranes are commonly linked to terrestrial higher plants and algae (Volkman 2005; Liu et al. 2021). To assess the contributions of lower organisms and higher plants in the samples, the regular sterane ratio, $C_{27}\text{ST}/C_{29}\text{ST}$, was examined, with the results presented in Table 4. Consistent with the Van Krevelen plot (Fig. 2c–d), the Paleocene samples exhibit a significantly lower $C_{27}\text{ST}/C_{29}\text{ST}$ ratio (0.64–0.82), suggesting a relatively lower proportion of lower aquatic organism precursors and a higher proportion of terrestrially sourced organic matter. Furthermore, a triangular plot of $C_{27–29}$ regular steranes, following established templates (Huang and Meinschein 1979; Volkman 1986; Liu et al. 2017), unambiguously indicates that the organic matter in the Paleocene samples

from the Tano Basin originates from mixed sources, with a predominance of land plants.

Additionally, stable carbon isotope ratios are invaluable tools for determining the sources, geological history, and depositional settings of organic matter within source rocks and crude oils (Maslen et al. 2011; Xinjian et al. 2017; Konan et al. 2022). Tissot and Welte (1984) observed that oils or source rocks containing terrigenous organic matter tend to have lighter isotopic values compared to marine oils. Furthermore, there is a gradual enrichment in ^{13}C as compound polarity increases (Stahl 1979; Chung et al. 1981). This suggests that the isotopic composition of hydrocarbons can provide valuable information about the origin and characteristics of the organic matter in a given sample. Specifically, the $\delta^{13}\text{C}$ values of oils and source rocks can be used to differentiate between marine and non-marine sources and to evaluate the hydrocarbon generation potential of a formation. The Paleocene mudstones from the Tano Basin exhibit a mixed source of organic matter with a high terrestrial component based on the heavier isotope signature present in Table 6. This conclusion is supported by previous studies by Tissot and Welte (1984), Mello et al. (1988), Maslen et al. (2011), and Konan et al. (2022). Maslen et al. (2011) reported that oils with isotope values above $-26\text{\textperthousand}$ are associated with terrestrial sources, while those with values below $-26\text{\textperthousand}$ primarily

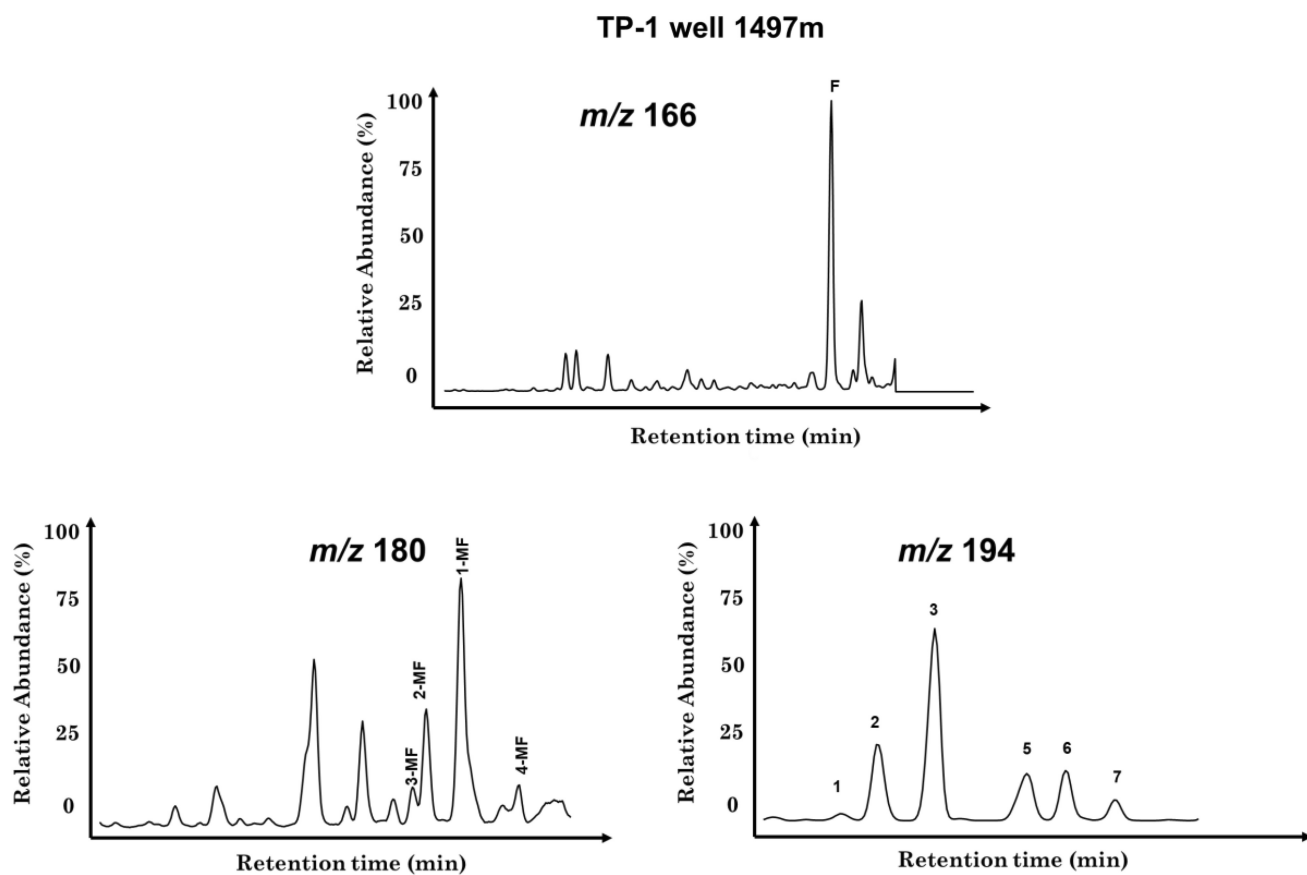


Fig. 10 **a** Representative aromatic hydrocarbon fraction mass chromatograms (m/z 166) showing fluorene **b** Representative aromatic hydrocarbon fraction mass chromatograms (m/z 180) showing methyl fluorene **c** Representative aromatic hydrocarbon fraction mass chromatograms (m/z 194) showing dimethyl fluorene in Paleocene mudrock samples from TP-1 well, Tano Basin

Table 5 Relative abundance of dibenzothiophene (DBT), fluorenes (F), and dibenzofuran (DBF) for evaluating the depositional environment of organic matter in Paleocene mudrock samples from TP-1 Well, Tano Basin

Sample ID	Strata	Well	Depth	Sample Type	Lithology	F (%)	DBT (%)	DBF (%)
T1	Paleocene	TP-1	975	Cuttings	Claystone	29.15	31.02	39.84
T2	Paleocene	TP-1	1050	Cuttings	Claystone	21.39	34.04	44.59
T3	Paleocene	TP-1	1113	Cuttings	Claystone	13.62	37.06	49.33
T4	Paleocene	TP-1	1190	Cuttings	Claystone	22.06	30.62	47.33
T5	Paleocene	TP-1	1250	Cuttings	Claystone	25.60	30.82	43.58
T6	Paleocene	TP-1	1300	Cuttings	Claystone	24.17	29.01	46.83
T7	Paleocene	TP-1	1341	Cuttings	Claystone	22.73	27.20	50.07
T8	Paleocene	TP-1	1433	Cuttings	Claystone	24.40	28.39	47.21
T9	Paleocene	TP-1	1460	Cuttings	Claystone	26.08	29.59	44.35
T10	Paleocene	TP-1	1497	Cuttings	Claystone	23.00	28.15	48.85

originate from marine sources. Konan et al. (2022) demonstrated that oils from mixed sources generally fall within the range of -28% to -20% , reflecting varying contributions from marine and terrestrial sources. Thus, the stable carbon isotope ratios in the Paleocene samples suggest a mixed source of organic matter with a stronger terrestrial input. This finding is consistent with the biomarker results.

5.2 Depositional environment

The Pr/Ph ratio serves as a valuable parameter for assessing redox conditions in the depositional environment and understanding organic matter composition (Didyk et al. 1978; Ten Haven et al. 1987; Zhang and Huang 2005; Duan et al. 2008). It relies on the concept that pristane primarily forms from phytol through oxidative processes,

Table 6 Stable carbon isotope ratios of saturated and aromatic fractions in Paleocene mudrock samples from TP-1 Well, Tano Basin

Sample ID	Strata	Well	Depth	Sample Type	Lithology	Component $\delta^{13}\text{C}_{\text{PDB}}(\text{\textperthousand})$		
						Sat	Aro	$\Delta\delta_{\text{Aro}} - \Delta\delta_{\text{Sat}}$
T1	Paleocene	TP-1	975	Cuttings	Claystone	– 28.18	– 26.63	1.55
T2	Paleocene	TP-1	1050	Cuttings	Claystone	– 28.02	– 26.53	1.50
T3	Paleocene	TP-1	1113	Cuttings	Claystone	– 27.86	– 26.42	1.44
T4	Paleocene	TP-1	1190	Cuttings	Claystone	– 27.77	– 26.99	0.77
T5	Paleocene	TP-1	1250	Cuttings	Claystone	– 27.67	– 27.56	0.11
T6	Paleocene	TP-1	1300	Cuttings	Claystone	– 27.85	– 27.04	0.80
T7	Paleocene	TP-1	1341	Cuttings	Claystone	– 28.02	– 26.53	1.50
T8	Paleocene	TP-1	1433	Cuttings	Claystone	– 27.85	– 27.04	0.80
T9	Paleocene	TP-1	1460	Cuttings	Claystone	– 27.67	– 27.56	0.11
T10	Paleocene	TP-1	1497	Cuttings	Claystone	– 27.88	– 26.92	0.95

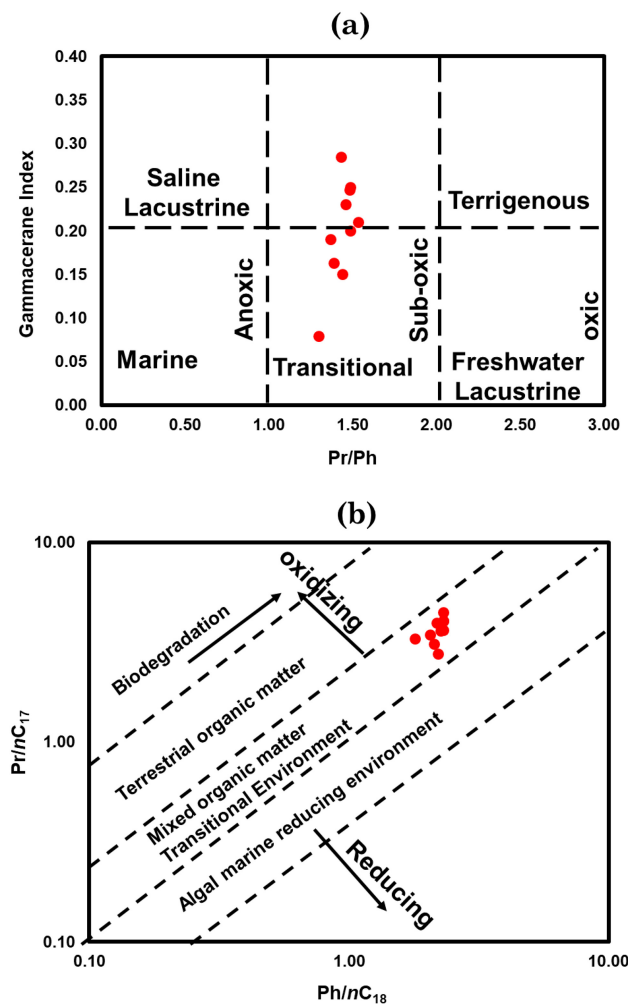


Fig. 11 **a** Cross plot Pr/Ph versus G/C_{30} HOP. Note: HOP: $\text{C}_{30} 17\alpha(\text{H}), 21\beta(\text{H})\text{-hopane}$ (after Tao et al. 2015) **b** Cross plot of Pr/nC_{17} ratio and Ph/nC_{18} ratios in Paleocene mudrock samples from TP-1 well, Tano Basin

while phytane results from various reductive pathways. Typically, a Pr/Ph ratio below 1.0 indicates a strongly reducing environment, while a ratio exceeding 3.0 suggests

an oxidizing environment. Ratios between 1.0 and 3.0 suggest suboxic redox conditions.

Gammacerane is a biomarker associated with the precursor tetrahymanol and is commonly found in hypersaline paleoenvironments (Henderson and Steel 1971). Recent studies have suggested that gammacerane originates from tetrahymanol and is typically present in saline waters (Fu and Sheng 1989; Sinnige Damste et al. 1995; Yu et al. 2011). In the Paleocene mudrocks from the Tano Basin, the relationship between the Pr/Ph ratios and the gammacerane index ($\text{G}/\text{C}_{30} \alpha\beta$ hopane) reveals a pattern that suggests a variable water salinity column (Fig. 11a). Pr/Ph ratios ranging between 1.3 and 1.5 suggest deposition in a sub-oxic redox condition within a transitional environment. Meanwhile, gammacerane index values varying between 0.8 and 0.28 indicate that the deposition of these mudrocks occurred in a stratified water column (Fig. 11a).

Furthermore, the distribution of Tricyclic (TTs) and tetracyclic (TeT) terpanes serves as a diagnostic biomarker for discriminating source rocks and crude oils from different sedimentary environments (Ekweozor and Strausz 1983; Xiao et al. 2018, 2019). In marine or saline lacustrine source rocks and their associated oils, it is common to observe a prevalence of C_{23}TT among $\text{C}_{19}\text{-}\text{C}_{23}\text{TT}$ homologs (Aquino Neto et al. 1983; Chen et al. 2017). Previous research by Peters and Moldowan (1993) proposed that terrigenous oils tend to have a higher abundance of C_{19} and C_{20} tricyclic terpanes. Conversely, crude oils with a marine source often exhibit a predominance of the C_{23} tricyclic terpane homolog. Longer chain tricyclic terpanes ($\text{C}_{19}\text{TT-C}_{33}\text{TT}$) are observed in marine and lacustrine crude oils (Xiao et al. 2021), while coal samples typically exhibit a high abundance of C_{19}TT (Zhu 1997; Fu et al. 2019). The origin of C_{24} tetracyclic terpanes (TeT) is still under investigation, but it is hypothesized that these biomarkers may arise from the thermal or microbial degradation of hopanes (Tao et al. 2015). Other studies have suggested

Table 7 Selected tricyclic terpane (TT), tetracyclic terpane (TeT) and hopanes for evaluating the depositional environment of organic matter in Paleocene mudrock samples from TP-1 Well, Tano Basin

Sample ID	Strata	Well	Depth	Sample type	Lithology	$(C_{19}TT + C_{20}TT)/C_{23}TT$	$C_{23}TT/C_{21}TT$	$C_{24}TeT/C_{26}TT$	$C_{25}TT/C_{24}TeT$	$C_{24}TeT/(C_{24}TeT + C_{26}TT)$	$C_{29}TT/C_{30}HOP$	$C_{28}TT/C_{30}HOP$
T1	Paleocene	TP-1	975	Cuttings	Claystone	1.31	1.28	1.55	0.62	0.61	0.30	0.02
T2	Paleocene	TP-1	1050	Cuttings	Claystone	1.20	1.44	1.57	0.63	0.61	0.25	0.02
T3	Paleocene	TP-1	1113	Cuttings	Claystone	1.14	1.52	1.58	0.63	0.61	0.22	0.02
T4	Paleocene	TP-1	1190	Cuttings	Claystone	1.12	1.43	1.60	0.71	0.62	0.19	0.03
T5	Paleocene	TP-1	1250	Cuttings	Claystone	0.93	1.58	1.65	0.79	0.62	0.08	0.03
T6	Paleocene	TP-1	1300	Cuttings	Claystone	1.08	1.60	1.59	0.64	0.61	0.19	0.03
T7	Paleocene	TP-1	1341	Cuttings	Claystone	1.06	1.51	1.61	0.71	0.62	0.16	0.03
T8	Paleocene	TP-1	1433	Cuttings	Claystone	0.84	1.91	1.63	0.65	0.62	0.08	0.03
T9	Paleocene	TP-1	1460	Cuttings	Claystone	0.89	1.75	1.64	0.72	0.62	0.08	0.03
T10	Paleocene	TP-1	1497	Cuttings	Claystone	0.93	1.58	1.65	0.79	0.62	0.08	0.03

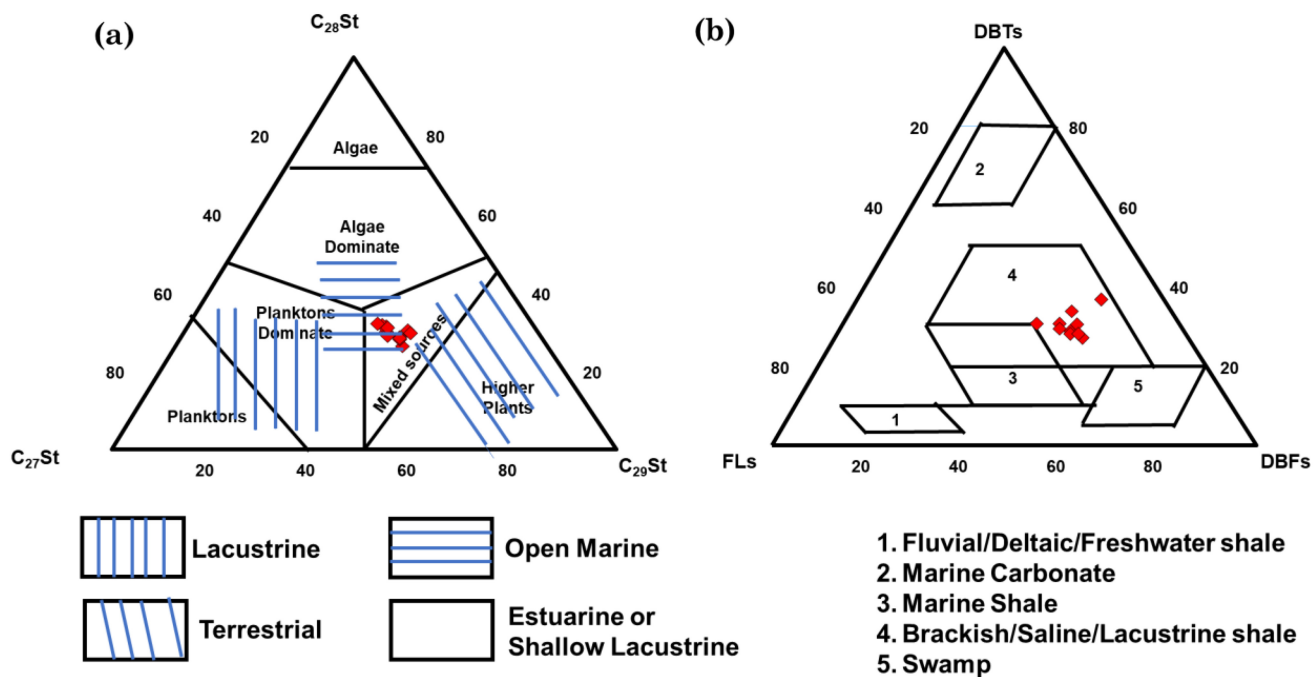


Fig. 12 **a** Ternary plot of C_{27} - C_{29} sterols showing the source input and depositional environment of organic matter (after Huang and Meinschein 1979; Volkman 1986; Liu et al. 2017) **b** Ternary plot of fluorenes (FLs), dibenzothiophene (DBTs) and dibenzofurans (DBFs) showing the depositional environment of organic matter in Paleocene mudrock samples from TP-1 well, Tano Basin (After Li et al. 2012)

that a high tetracyclic to tricyclic terpane ratio is characteristic of terrestrial settings (Aquino Neto et al. 1983). Thus, tricyclic terpanes provide valuable insights into the depositional environments of source rocks and their associated oils, aiding in understanding hydrocarbon generation and exploration in diverse geological settings. Consistent with the changing distribution of regular steranes shown in Table 4 and the gammacerane index values in Table 2, the variations in the tricyclic terpane ratio ($C_{19}\text{TT} + C_{20}\text{TT}/C_{23}\text{TT}$) depicted in Fig. 13a and Table 7 suggest that these mudrocks were deposited in a transitional environment, where freshwater mixes with saline water.

Recent research has demonstrated that the relative abundances of fluorenes, dibenzofurans, and dibenzothiophenes (FL, DBT, and DBF) can provide valuable information about the depositional environment of sedimentary rocks (Li et al. 2004, 2011, 2013). For example, oils from marine and saline lake environments tend to have higher contents of dibenzothiophene, while oils from freshwater and brackish lakes are often dominated by fluorene (Li et al. 2012). The relative abundance of DBT, DBF, and FL in the Paleocene mudrock samples from the Tano Basin is presented in Table 5. The triplot of DBT, DBF, and FL in Fig. 12b suggests that the organic matter in the Paleocene samples from the Tano Basin was deposited in a transitional environment (Li et al. 2012). This conclusion is consistent with the $C_{27}^-C_{29}$ regular sterane triangular plot

(Fig. 12a), gammacerane index (Fig. 11a), and tricyclic terpane ratios (Fig. 13a).

5.3 Comprehensive thermal maturity assessment

The quality of source rocks is influenced by several factors, including the type and abundance of organic matter, as well as their organic richness and thermal maturity. In this section, we focus on assessing the thermal maturity of the organic matter in the Paleocene mudrocks, examining both their kerogen maturity (T_{\max}) and molecular maturity parameters.

As a screening parameter, T_{\max} values below 435–440 °C are associated with immature or early mature source rocks, while in the mid-maturity range, T_{\max} typically falls within the range of 435–445 °C. As thermal maturation progresses, T_{\max} values gradually increase (Peters and Cassa 1994). The T_{\max} range of (405–436 °C) in the samples suggests an immature to mid-maturity range (Fig. 2f).

Molecular parameters, namely $T_s/(T_s + T_m)$ ratios, $C_{31}\text{HH22S}/(22S + 22R)$, and $C_{29}\text{St20S}/(20S + 20R)$, have been demonstrated to be highly responsive indicators of organic matter maturation within the saturated hydrocarbon fraction of rock extracts and crude oils (Scalan and Smith 1970; Seifert and Moldowan 1986; Peters et al. 2005). The $T_s/(T_s + T_m)$ ratio represents the relative abundance of 18 α (H)-22,29,30-trinorhopane (T_s) to

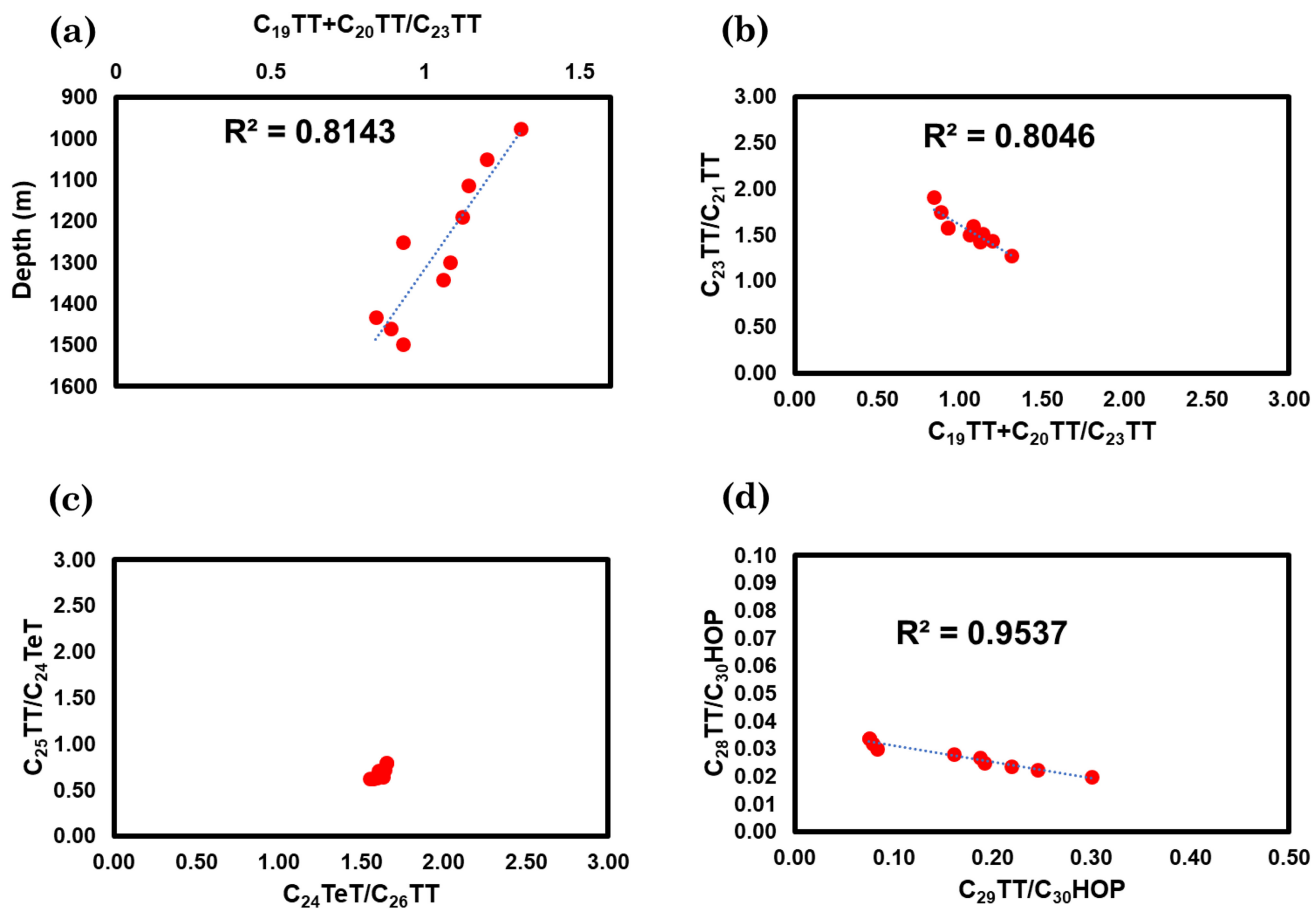


Fig. 13 **a** Plot of $C_{19}\text{TT} + C_{20}\text{TT}/C_{23}\text{TT}$ with depth suggests depositional environment of the Paleocene mudrocks from the Tano Basin fluctuates between marine and freshwater environment **b** Variation of $C_{23}\text{TT}/C_{21}\text{TT}$ versus $C_{19}\text{TT} + C_{20}\text{TT}/C_{23}\text{TT}$ suggests depositional environment of the Paleocene mudrocks from the Tano Basin fluctuates between marine and freshwater environment **c** Plot of $C_{25}\text{TT}/C_{24}\text{TeT}$ versus $C_{24}\text{TeT}/C_{26}\text{TT}$ shows the dominance of terrestrial organic matter input in Paleocene mudrock samples from TP-1 well, Tano Basin. **d** Plot of $C_{28}\text{TT}/C_{30}\text{HOP}$ versus $C_{29}\text{TT}/C_{30}\text{HOP}$ shows the low abundance of longer chain tricyclic terpanes in Paleocene mudrock samples from TP-1 well, Tano Basin

$17\alpha(\text{H})$ -22,29,30-trinorhopane (Tm) and is influenced by both the maturity and source facies of the samples. Although the specific value of this ratio heavily relies on the initial facies of the samples, it tends to reach a stable equilibrium during intermediate to advanced stages of thermal maturity (Peters et al. 2005; Gao et al. 2007). In the case of the Paleocene samples under study, the observed Ts/(Ts + Tm) ratios show an increasing trend with depth (ranging from 0.2 to 0.39), implying a progressive thermal maturation of these rocks with increasing depth (Fig. 14a).

Moreover, in the immature to early stages of oil generation, $C_{31-35}\text{HH22S}/(22\text{S} + 22\text{R})$ ratios have been identified as valuable maturity parameters (Peters et al. 2005). Typically, these ratios range from 0.50 to 0.54 during the early oil generation phase and increase to between 0.57 and 0.62 during the main oil generation phase. However, the $22\text{S}/(22\text{S} + 22\text{R})$ ratio remains

constant after reaching isomerization equilibrium, leading to a lack of additional maturity information (Seifert and Moldowan 1986; Peters et al. 2005). In contrast to the Ts/(Ts + Tm) maturity parameter, the plot of $C_{31}\text{HH22S}/(22\text{S} + 22\text{R})$ versus $C_{29}\text{20S}/(20\text{S} + 20\text{R})$, as shown in Fig. 14b, clearly indicates that the Paleocene samples are currently in the immature phase of oil generation.

Similarly, aromatic molecular markers are commonly used alongside saturated molecular markers to assess source rock maturity due to their superior stability. Among these, the alkyl phenanthrene and alkyl naphthalene ratios are extensively employed as molecular maturity parameters in the aromatic fractions (Radke et al. 1982, 1986; Yuzhuang et al. 2005; Asif et al. 2011). Table 3 provides a comprehensive compilation of eleven molecular ratios derived from both saturated and aromatic hydrocarbon fractions, serving as maturity parameters to evaluate the organic maturation levels of the Paleocene mudstones.

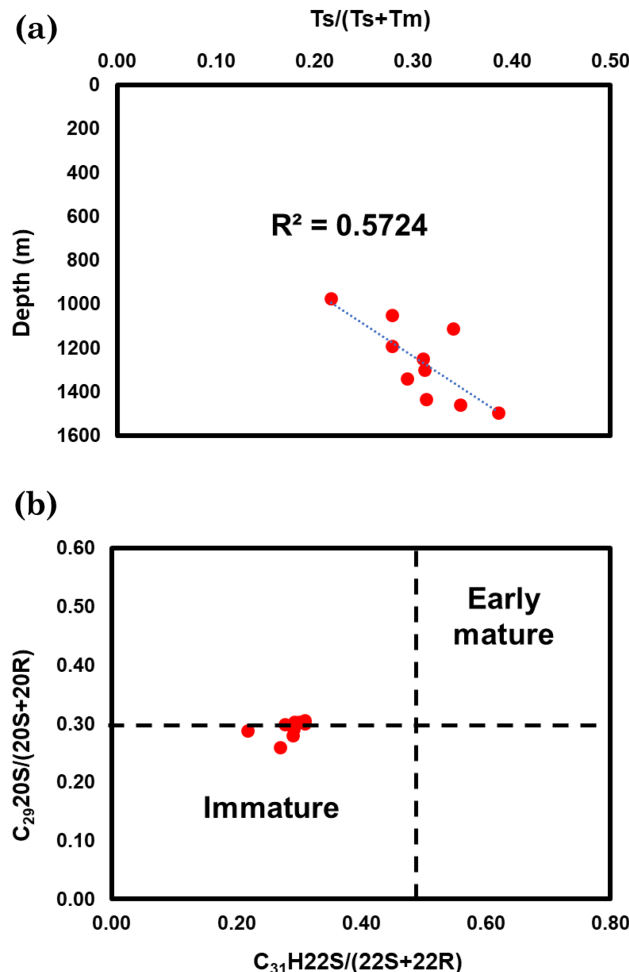


Fig. 14 **a** Depth profile of $Ts/(Ts + Tm)$ shows the maturity of organic matter in the Paleocene samples from TP-1 well, Tano Basin, increases with depth **b** Plot of $C_{31}HH22S/(22S + 22R)$ versus $C_{29}20S/(20S + 20R)$ indicates the immaturity of Paleocene samples

Two parameters, MPI-1 (methylphenanthrene index) and MPI-2 [$3*(2\text{-methyl phenanthrene})]/[\text{phenanthrene} + (1\text{-methyl phenanthrene}) + (9\text{-methyl phenanthrene})]$, exhibit a good maturity range with depth within the Paleocene samples of the Tano Basin; however, the remaining 6 aromatic maturity parameters do not show consistent or distinct variations with depth (Fig. 15). The computed vitrinite reflectance (R_c) of the Paleocene samples, based on the methyl phenanthrene index formula ($R_c = 0.6MPI - 1 + 0.4$, Radke et al. 1982), ranges from 0.65% to 0.76%. This indicates that the Paleocene samples are in the main oil generation phase (Peters and Cassa 1994).

To sum up, we have observed a consistent trend of increasing organic matter maturity in the Paleocene source strata with depth based on the analysis of bulk and molecular maturity parameters.

6 Regional correlations with other basins

This section offers a comparative analysis of Paleocene source rocks in the Tano Basin with those in other basins along the West and South Atlantic margins. These basins include the Niger Delta Basin, Douala and Kribi-Campo Basins in Cameroon, the Kwanza Formation in Angola, and some basins in the northern part of the Brazilian margin. It is noteworthy that the geological and tectonic histories of the Brazilian and West African continental margins share similarities due to their proximity during and after the separation of Africa and South America in the Late Jurassic to Late Cretaceous period. As a result, rift and marginal basins in both continents exhibit correlations (Schiefelbein et al. 2000).

Bustin (1988) and Tuttle et al. (1999) demonstrated that the Paleocene source rocks in the Niger Delta Basin primarily consist of Type II/III kerogen and originate from marine sources. The total organic carbon (TOC) content in these rocks ranges from 1 to 2 wt%. Varying degrees of thermal maturity are observed in these rocks, spanning from marginally mature to late mature (Odumodu and Mode 2016).

Recent research by Wotanie et al. (2022) and Nijoh and Sama (2022) has highlighted that the Paleocene source unit in the Douala Basin and Kribi-Campo Basins of Cameroon predominantly contains Type II and Type III kerogens. These sediments were deposited in nearshore/shallow marine paleo-depositional environments, characterized by a significant influx of continental debris. These rocks typically possess TOC content ranging from 0.5 to 2 wt% and are considered marginally mature (with vitrinite reflectance values, V_R , ranging from 0.50 to 0.59%).

In the Kwanza Basin, Angola, the Paleocene source strata within the Rio Dande Formation exhibit kerogen types II, II/I, and II/III, with TOC levels ranging from 2 to 10 wt%. The thermal maturity of these rocks varies from immature to mature, depending on the specific sampling location. According to Raposo and Inkollu (1998), the depositional environment of these Paleocene source rocks in the Kwanza Basin, Angola, is marine.

Furthermore, Mello et al. (1988) showed that Paleocene source rocks from the northern part of the Brazil marginal basins have a TOC content of up to 7 wt%, primarily arising from Type II/III kerogen, with thermal maturity ranging from immature to peak mature. The depositional environment of these rocks overlaps between marine and deltaic environments.

The correlation studies indicate that the Paleocene source rocks in the Tano Basin share similarities in terms of organic matter composition with those observed in the aforementioned basins (Fig. 16). However, there are

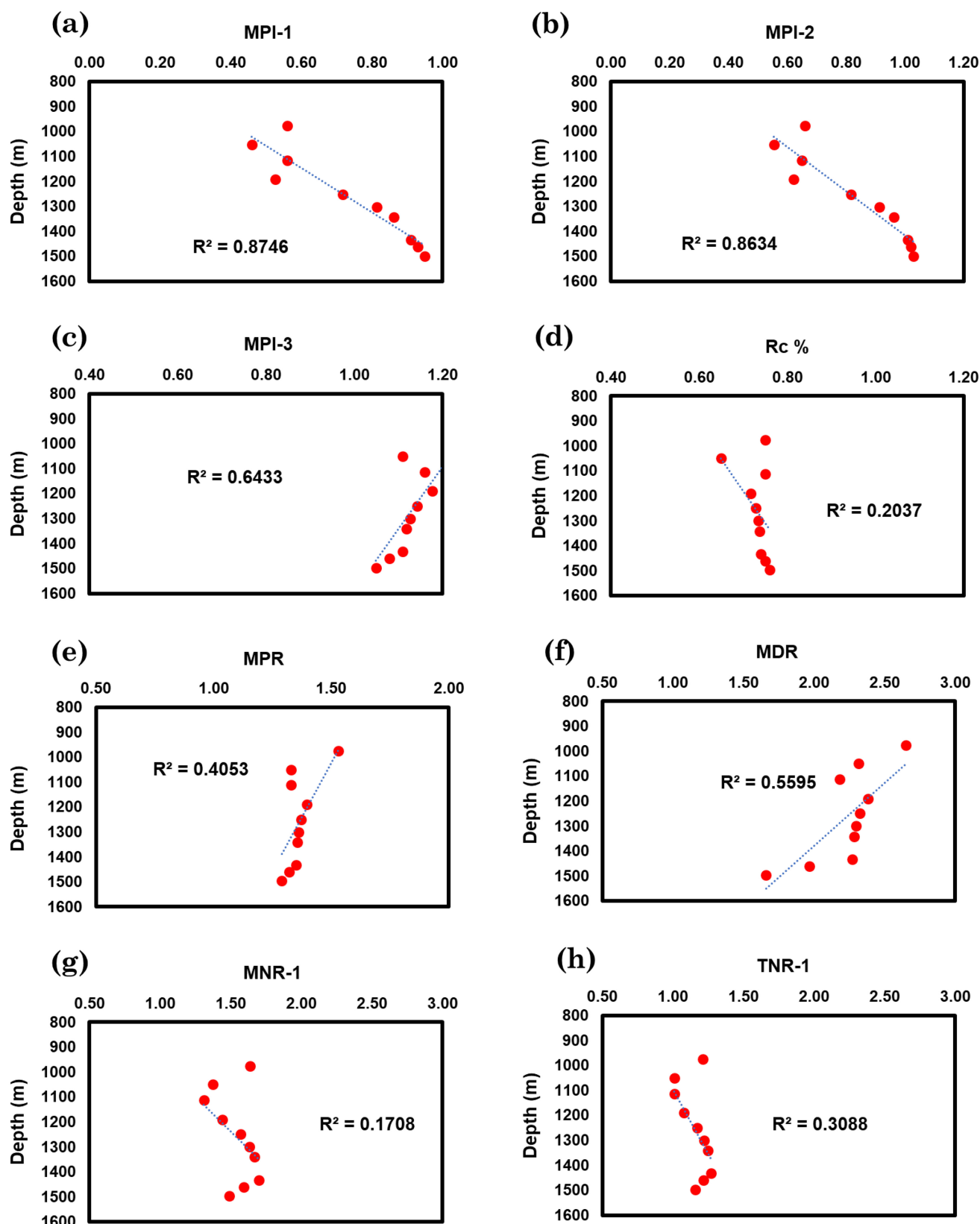


Fig. 15 Plot of some aromatic maturity parameters with depth showing the maturation range of organic matter in Paleocene mudrock samples from TP-1 well, Tano Basin

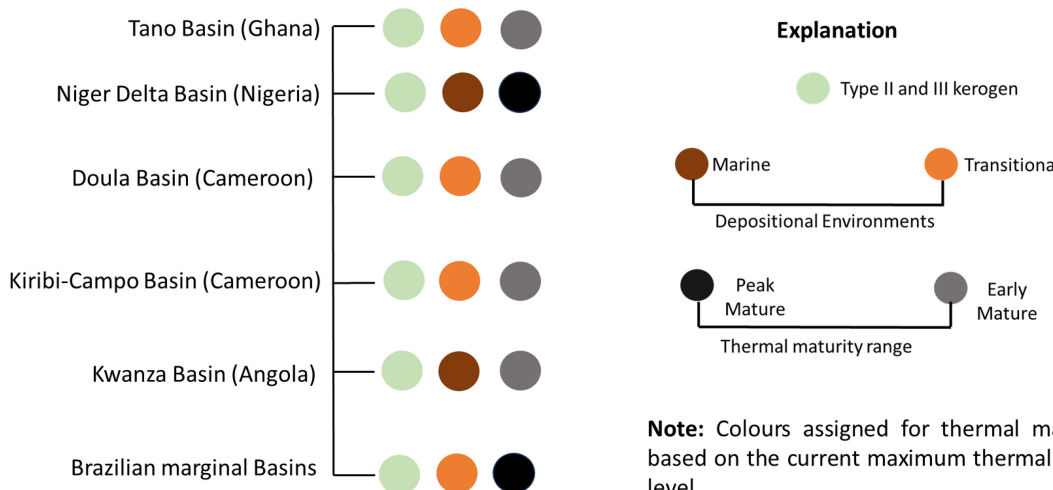


Fig. 16 Kerogen types, depositional environments, and organic matter thermal maturity in Paleocene Mudrocks of the Tano Basin and South Atlantic Marginal Basins

variations in the thermal maturity range of these rocks across regions, possibly attributable to differences in heat flow and burial history. For instance, source rocks in the Potiguar Basin in Brazil have undergone thermal maturity influenced by heat flow (da Silva et al. 2021). Currently, the thermal maturity of the Paleocene source rocks in the TP-1 well of the Tano Basin is relatively low compared to what is observed in the Niger Delta and the Brazilian marginal basins (Fig. 16). Ultimately, gaining a comprehensive understanding of the thermal maturity of the Paleocene source rocks in the Tano Basin may require extensive geochemical studies or basin modeling approaches.

7 Conclusion

This research aimed to investigate the unexplored petroleum potential and organic facies of the Paleocene source strata in the Tano Basin, an area that has received limited attention in prior exploration efforts. Through comprehensive geochemical analysis, including the assessment of total organic carbon content, Rock-Eval pyrolysis, biomarker, and isotopic analysis, the study has yielded the following conclusions:

The analysis reveals that the Paleocene mudrocks from the Tano Basin contain a combination of Type II and III kerogen, exhibiting organic richness ranging from lean to moderate. The presence of indigenous hydrocarbons originating from mixed sources underscores the significance of these rocks as potential source rocks. Furthermore, the study highlights the crucial role played by the sub-oxic transitional environment with variable salinity gradients in preserving the organic matter in these rocks. Maturity

assessment based on rock pyrolysis Tmax and biomarker ratios indicates that the organic matter within these mudrocks is in the immature to early mature phases in terms of oil generation, with maturity increasing with depth.

In comparison, the Paleocene source rocks in the Tano Basin share many similarities in terms of organic composition and depositional environments with those in the South Atlantic marginal basins, including the Niger Delta Basin, Douala and Kribi-Campo Basins in Cameroon, the Kwanza Formation in Angola, and certain basins in the northern part of the Brazilian margin. However, it is worth noting that the thermal maturity of the Tano Basin's Paleocene source rocks is relatively low compared to what is observed in the Niger Delta and the Brazilian marginal basins.

In conclusion, this study has unveiled the previously overlooked marginal hydrocarbon potential of Paleocene mudrocks in the Tano Basin. The shared geochemical characteristics between the Paleocene mudrocks of the Tano Basin and those in the South Atlantic marginal basins provide valuable insights into source rock quality, essential for informing future exploration endeavors in this region.

Acknowledgements The authors extend their heartfelt appreciation to the Ghana National Petroleum Company (GNPC) for providing invaluable samples and crucial information that greatly contributed to this study. Furthermore, we are sincerely grateful to the State Key Laboratory of Petroleum Resources and Prospecting at the China University of Petroleum, Beijing (CUPB), for generously funding all the geochemical tests conducted during this research. We would also like to express our gratitude to Dr. Qingyong Luo, and Dr. Wang Guangli of CUPB for their invaluable technical support and insightful comments on our paper, which significantly enhanced the quality of our work.

Author contributions Conceptualization: KA and ZN. Data curation: KA. Formal analysis: KA, NPO-B, NFDeSK, SS. Funding acquisition: ZN. Investigation: KA, NPO-B. Methodology: KA, SS, NPO-B. Project administration: ZN. Resources: ZN, EA, CF, GF. Software: SS. Supervision: ZN. Validation: SS, ZN, KA, NPO-B, EA, CF. Writing—original draft: KA. Writing—review and editing: ZN, POA, GF, CF, EA. All authors have read and agreed to the published version of the manuscript.

Funding This work is a segment of the corresponding author's master's thesis, and the expenses related to this research were funded by the State Key Petroleum Lab of Petroleum Resources and Prospecting at China University of Petroleum (Beijing).

Data availability Not applicable.

Declarations

Conflict of interest The authors declare no conflict of interest.

References

- Abubakar R, Adomako-Ansah K, Marfo SA, Owusu JA, Fenyi C (2022) Origin and depositional environment of oils and sediments in the Cretaceous Deep-Water Tano Basin, Ghana: constraints from biomarkers. *Petrol Sci Technol*. <https://doi.org/10.1080/10916466.2022.2143804>
- Akaba PA, Owusu JA, Apesegah E, Takyi B, Bempong FK, Foli G, Gawa SK (2022) Spatiotemporal evolution of potential source rocks in the Cretaceous stratigraphic units, Offshore Ghana. *Pet Coal* 64:20–33
- Amoako K, Ningning Z, Osei-Boakye NP, Konan NGFDS, Foli G, Appau PO, Apesegah E (2023) Molecular and isotopic signatures of indigenous and non-indigenous hydrocarbons in Campanian sediments from the Tano Basin, Ghana. *Appl Geochem* 155:105719
- Aquino NF (1983) Occurrence and formation of tricyclic and tetracyclic terpanes in sediments and petroleum. *Adv Org Geochem* 1981:659–667
- Asif M, Nazir A, Fazeelat T, Grice K, Nasir S, Saleem A (2011) Applications of polycyclic aromatic hydrocarbons to assess the source and thermal maturity of the crude oils from the Lower Indus Basin, Pakistan. *Pet Sci Technol* 29:2234–2246. <https://doi.org/10.1080/10916461003699226>
- Atta-Peters D, Garrey P (2014) Source rock evaluation and hydrocarbon potential in the Tano Basin, South Western Ghana, West Africa. *Int J Oil Gas Coal Eng* 2:66–77. <https://doi.org/10.11648/j.ogce.20140205.11>
- Atta-Peters D, Salami MB (2004) Campanian to Paleocene dinoflagellate cyst biostratigraphy from offshore sediments in the Tano Basin, southwestern Ghana. *Rev Esp Micropaleontol* 36:305–321
- Beglinter SE, Doust H, Cloetingh S (2012a) Relating petroleum system and play development to basin evolution: West African South Atlantic basins. *Mar Pet Geol* 30:1–25
- Beglinter SE, Doust H, Cloetingh S (2012b) Relating petroleum system and play development to basin evolution: Brazilian South Atlantic margin. *Pet Geosci* 18:315–336
- Bempong FK, Ozumba BM, Hotor V, Takyi B, Nwanjide CS (2019) A review of the geology and the petroleum potential of the Cretaceous Tano Basin of Ghana. *J Pet Environ Biotechnol* 10:1–6
- Bilal A, Yang R, Lenhardt N, Han Z, Luan X (2023a) The Paleocene Hangu formation: a key to unlocking the mysteries of Paleo-Tethys tectonism. *Mar Petrol Geol* 157:106508
- Bilal A, Yang R, Janjuhah HT, Mughal MS, Li Y, Kontakiotis G, Lenhardt N (2023b) Microfacies analysis of the Palaeocene Lockhart limestone on the eastern margin of the Upper Indus Basin (Pakistan): implications for the depositional environment and reservoir characteristics. *Depos Record* 9:152–173
- Brownfield ME, Charpentier RR (2006) Geology and total petroleum systems of the West-Central Coastal province 7203, West Africa, Report 2207-B, US Geological Survey Bulletin, pp 59
- Bustin M (1988) Sedimentology and characteristics of dispersed organic matter in Tertiary Niger Delta. Origin of source rocks in a Deltaic environment. *Am Assoc Pet Geol Bull* 72:277–298
- Carvajal-Ortiz H, Gentzis T (2015) Critical considerations when assessing hydrocarbon plays using Rock-Eval pyrolysis and organic petrology data: data quality revisited. *Int J Coal Geol* 152:113–122. <https://doi.org/10.1016/j.coal.2015.06.001>
- Chang XC, Wang Y, Shi BB, Xu YD (2019) Charging of Carboniferous volcanic reservoirs in the eastern Chepaizi Uplift, Junggar Basin NW China is constrained by oil geochemistry and fluid inclusion. *AAPG Bull*. <https://doi.org/10.1306/12171818041>
- Chen ZL, Liu GD, Wei YZ, Gao G, Ren JL, Yang F, Ma WY (2017) Distribution pattern of tricyclic terpanes and its influencing factors in the Permian source rocks from Mahu depression in the Junggar Basin. *Oil Gas Geol* 38:2:12
- Chen ZH, Wang TG, Li MJ, Yang FL, Cheng B (2018) Biomarker geochemistry of crude oils and lower paleozoic source rocks in the Tarim Basin, western China: an oil source rock correlation study. *Mar Pet Geol* 96:94–112
- Chung HM, Brand SW, Grizzell PL (1981) Carbon isotope geochemistry of Paleozoic oils from Big Horn Basin. *Geochim Cosmochim Acta* 45:1803–1815. <https://doi.org/10.1016/0016-70378190011-9>
- Connan J, Cassou AM (1980) Properties of gases and petroleum liquids derived from terrestrial kerogen at various maturation levels. *Geochim Cosmochim Acta* 44:1–23
- Curiale J, Bromley B (1996) Migration-induced compositional changes in oils and condensates of a single field. *Org Geochem* 24:1097–1113. <https://doi.org/10.1016/S0146-63809600099-X>
- da Silva EB, Ribeiro HJS, de Souza ES (2021) Exploration plays of the Potiguar Basin in deep and ultra-deep water, Brazilian Equatorial Margin. *J S Am Earth Sci* 111:103454
- Didyk BM, Simoneit BRT, Brassell SC, Eglington G (1978) Organic geochemical indicators of palaeoenvironmental conditions of sedimentation. *Nature* 272:216–222
- Duan Y, Wang CY, Zheng CY, Wu BX, Zheng GD (2008) Geochemical study of crude oils from Xifeng oilfield of Ordos Basin, China. *J Asian Earth Sci* 31:341–356
- Ekweozor CM, Strausz OP (1983) Tricyclic terpanes in the Athabasca oil sands: their geochemistry. *Adv Org Geochem* 1981:746–766
- Eisenlohr BN, Hirdes W (1992) The structural development of the early Proterozoic Birimian and Tarkwaian rocks of southwest Ghana, West Africa. *J. African Earth Sci (and the Middle East)* 14(3): 313–325
- Espariaté J, Madec M, Tissot B, Mennig JJ, Leplat P (1977) Source rock characterization method for petroleum exploration. In: Paper presented at the Offshore Technology Conference, Houston, pp 439–444. <https://doi.org/10.4043/2935-MS>
- Fu JM, Sheng GY (1989) Biological marker composition of typical source rocks and related oils of terrigenous origin in the People's Republic of China: a review. *Appl Geochem* 4:13–22
- Fu J, Zhang Z, Chen C, Wang TG, Li M, Ali S, Xiaolin L, Dai J (2019) Geochemistry and origins of petroleum in the Neogene reservoirs of the Baiyun Sag, Pearl River Mouth Basin. *Mar Pet Geol* 107:127–141

- Gao X, Chen S, Xie X, Long A, Ma F (2007) Non-aromatic hydrocarbons in surface sediments near the Pearl River estuary in the South China Sea. *Environ Pollut* 148:40–47. <https://doi.org/10.1016/j.envpol.2006.11.001>
- Garry P, Atta-Peters D, Achaegakwo C (2016) Source-rock potential of the lower cretaceous sediments in SD-1X well, offshore Tano Basin, south western Ghana. *Pet Coal* 58:476–489
- Gough MA, Rowland SJ (1990) Characterization of unresolved complex-mixtures of hydrocarbons in petroleum. *Nature* 344:648–650. <https://doi.org/10.1038/344648a0>
- Henderson W, Steel G (1971) Isolation and characterization of triterpenoid alcohol from Green River Shale. *J Chem Soc Chem Commun* 21:1331–1332
- Huang WY, Meinschein WG (1979) Sterols as ecological indicators. *Geochim Cosmochim Acta* 43:739–745
- Hunt JM (1966) The significance of carbon isotope variations in marine sediments. In: *Advances in organic geochemistry. Proceedings of the third international congress*, London, pp 27–35
- Jarvie DM (1991) Total organic carbon TOC analysis: Chapter 11: geochemical methods and exploration. In: Merill RK (ed) *Source and migration processes and evaluation techniques*. American Association of Petroleum Geologists, pp 113–118. <https://doi.org/10.1306/TrHbk543C11>
- Kelly J, Doust H (2016) Exploration for late cretaceous turbidites in the equatorial African and northeast South American margins. *Neth J Geosci* 95:393–403
- Kesse GO (1985) The mineral and rock resources of Ghana
- Konan NGFDS, Li M, Shi S, Kojo A, Toyin A, Boakye NPO, Li T (2022) Stable carbon isotopic composition of selected Alkyl-naphthalenes and Alkylphenanthrenes from the Tarim Oilfields. *NW China Energies* 15:7145. <https://doi.org/10.3390/en15197145>
- Lake S, Derewetsky A, Frewin N (2014) Structure, evolution, and petroleum systems of the Tano Basin, Ghana
- Li JG, Li M, Wang ZY (2004) Dibenzofuran series in terrestrial source rocks and crude oils and applications to oil-source rock correlations in the Kuche Depression of Tarim Basin, NW China. *Chin J Geochem* 23:113–123. <https://doi.org/10.1007/BF02868974>
- Li MJ, Wang TG, Yang FL, Shi Y (2011) Molecular tracers for filling pathway in condensate pools: alkylbenzofuran. *J. Oil Gas Technol. J Jianghan Petrol Inst* 33:6–11
- Li M, Wang TG, Lillis PG, Wang C, Shi S (2012) The significance of 24-norcholestanes, triaromatic steroids and dinosteroids in oils and Cambrian-Ordovician source rocks from the cratonic region of the Tarim Basin, NW China. *Appl Geochem* 27:1643–1654
- Liu B, Bechtel A, Sachsenhofer RF, Gross D, Gratzer R, Chen X (2017) Depositional environment of oil shale within the second member of permian Lucaogou formations in the Santanghu basin, Northwest China. *Int J Coal Geol* 175:10–25
- Liu M, Ji C, Hu H, Xia G, Yi H, Them TR, Sun P, Chen D (2021) Variations in microbial ecology during the Toarcian oceanic anoxic event Early Jurassic in the Qiangtang Basin, Tibet: evidence from biomarker and carbon isotopes. *Palaeogeogr Palaeoclimatol Palaeoecol* 580:110626
- Maslen E, Grice K, Le Métayer P, Dawson D, Edwards D (2011) Stable carbon isotopic compositions of individual aromatic hydrocarbons as source and age indicators in oils from western Australian basins. *Org Geochem* 42:387–398. <https://doi.org/10.1016/j.orggeochem.2011.02.005>
- Mello MR, Telnaes N, Gaglianone PC, Chicarelli MI, Brassell SC, Maxwell JR (1988) Organic geochemical characterization of depositional palaeoenvironments of source rocks and oils in Brazilian marginal Basins. In: *Organic geochemistry in petroleum exploration*, pp 31–45
- Njoh OA, Sama N (2022) Palynostratigraphy of the Paleocene–Eocene Shallow marine petroleum source rock sections, outcropping in Missole, Nkapa Formation, Douala/Kribi-Campo Basin, Cameroon
- Odumodu CFR, Mode AW (2016) Hydrocarbon maturation modeling of Paleocene to lower Miocene source rocks in the Niger Delta Basin: implications for hydrocarbon generation. *Arab J Geosci* 9:1–14
- Ogbesejana AB, Liu B, Gao S, Akinyemi SA, Bello OM, Song Y (2023) Applying biomarkers as paleoenvironmental indicators to reveal the organic matter enrichment of shale during deep energy exploration: a review. *RSC Adv* 13:25635–25659
- Panford K (2022) Travails of Ghana's decade of crude oil production and exports: lessons and policy prescriptions. *Petroleum resource management in africa: lessons from 10 years of oil and gas production in Ghana*. Springer International Publishing, Cham, pp 483–520
- Peters KE, Moldowan JM (1993) The biomarker guide: interpreting molecular fossils in petroleum and ancient sediments. Prentice Hall, Englewood Cliffs
- Peters KE, Walters CC, Moldowan J (2005) The biomarker guide, vol 2. Cambridge University Press, Cambridge
- Peters KE, Cassa MR (1994) Applied source rock geochemistry. In: Magno LB, Dow WG (ed) *The Petroleum system-source to trap*. AAPG Memoir, pp 93–120. <https://doi.org/10.1306/M60585C5>
- Radke M, Welte DH, Willsch H (1982) Geochemical study on a well in the Western Canada Basin: relation of the aromatic distribution pattern to maturity of organic matter. *Geochim Cosmochim Acta* 46:1–10. <https://doi.org/10.1016/0016-70378290285-X>
- Radke M, Welte D, Willsch H (1986) Maturity parameters based on aromatic hydrocarbons: Influence of the organic matter type. *Org Geochem* 10:51–63. <https://doi.org/10.1016/0146-63808690008-2>
- Raposo A, Inkollu M (1998) Tertiary reservoirs in Congo-Kwanza-Namibe Basins. In: Mello MR, Yilmaz PO (ed) Rio '98—Petroleum geology in a changing world, November 8–11, 1998, Rio de Janeiro, Brazil, extended abstracts volume, pp 668–669
- Scalan E, Smith J (1970) An improved measure of the odd–even predominance in the normal alkanes of sediment extracts and petroleum. *Geochim Cosmochim Acta* 34:611–620
- Schiefelbein CF, Zumberge JE, Cameron NR, Brown SW (2000) Geochemical comparison of crude oil along the South Atlantic margin. In: Mello MR, Katz BJ (ed) *Petroleum systems of South Atlantic margins: American association of petroleum geologists memoir*, vol. 73, pp 15–26
- Seifert WK, Moldowan JM (1986) Use of biological markers in petroleum exploration. *Methods Geochem Geophys* 24:261–290
- Shanmugam G (1985) Significance of coniferous rainforests and related organic matter in generating commercial quantities of oil, Gippsland Basin, Australia. *AAPG Bull* 69:1241–1254
- Sinninghe Damste JS, Kenig F, Koopmans MP, Köster J, Schouten S, Hayes JM, de Leeuw JW (1995) Evidence for gammacerane as an indicator of water column stratification. *Geochim Cosmochim Acta* 59:1895–1900
- Stahl W (1979) Carbon isotopes in petroleum geochemistry. In: Jäger E et al (eds) *Lectures in isotope geology*. Springer-Verlag, Berlin Heidelberg, pp 274–282
- Ten Haven HL, De Leeuw JW, Rullkötter J, Damsté JS (1987) Restricted utility of the pristane/phytane ratio as a palaeoenvironmental indicator. *Nature* 330:641–643
- Tao S, Wang C, Du J, Liu L, Chen Z (2015). Geochemical application of tricyclic and tetracyclic terpanes biomarkers in crude oils of NW China. *Mar Pet Geol* 67: 460–467
- Tissot BP, Welte DH (1984) From kerogen to petroleum. In: *Petroleum formation and occurrence*. Springer, Berlin,

- Heidelberg, pp 160–198. https://doi.org/10.1007/978-3-642-87813-8_10
- Tuttle ML, Charpentier RR, Brownfield ME (1999) The Niger delta petroleum system: Niger delta province, Nigeria, Cameroon, and Equatorial Guinea, Africa, US Department of the Interior, US Geological Survey, pp 99–50
- Vandenbroucke M, Largeau C (2007) Kerogen origin, evolution and structure. *Org Geochem* 38:719–833
- Volkman JK (1986) A review of sterol markers for marine and terrigenous organic matter. *Org Geochem* 9:83–99
- Volkman JK (2005) Sterols and other triterpenoids: source specificity and evolution of biosynthetic pathways. *Org Geochem* 36:139–159
- Wotanie LV, Agyingi CM, Ayuk NE, Ngia NR, Anatole DL, Eble CF (2022) Petroleum source rock evaluation of organic black shales in the Paleogene N'kapa formation, Douala Basin, Cameroon. *Sci Afr* 18:e01437
- Xiao H, Wang TG, Li M, Fu J, Tang Y, Shi S, Lu X (2018) Occurrence and distribution of unusual tri-and tetracyclic terpanes and their geochemical significance in some Paleogene oils from China. *Energy Fuels* 32:7393–7403
- Xiao H, Li MJ, Yang Z, Zhu ZL (2019) Distribution patterns and geochemical implications of C19–C23 tricyclic terpanes in source rocks and crude oils occurring in various depositional environments. *Geochimica* 482:161–170. <https://doi.org/10.19700/j.0379-1726.2019.02.006>
- Xiao H, Wang T, Li M, You B, Zhu Z (2021) Extended series of tricyclic terpanes in the Mesoproterozoic sediments. *Org Geochem* 156:104245
- Xinjian ZHU, Jianfa CHEN, Jianjun WU, Yifan W, Zhang B, Zhang K, Liwen H (2017). Carbon isotopic compositions and origin of Paleozoic crude oil in the platform region of Tarim Basin, NW China. *Pet Explor Dev* 44(6): 1053–1060
- Yu QH, Wen ZJ, Tang YJ (2011) Geochemical characteristics of Ordovician crude oils in the northwest of the Tahe oil field, Tarim Basin. *Chin J Geochem* 30:93–98
- Yuzhuang S, Jinxi W, Luofu L, Jianping C (2005) Maturity parameters of source rocks from the Baise Basin, South China. *Energy Explor Exploit* 23:257–265
- Zhang SC, Huang HP (2005) Geochemistry of Palaeozoic marine petroleum from the Tarim Basin, NW China: Part 1. Oil Family Classification *Org Geochem* 36:1204–1214
- Zhu Y (1997) Geochemical characteristics of terrestrial oils of the Tarim Basin. *Acta Sedimentol Sin* 15:26–30 (**in Chinese with English abstract**)

Springer Nature or its licensor (e.g. a society or other partner) holds exclusive rights to this article under a publishing agreement with the author(s) or other rightsholder(s); author self-archiving of the accepted manuscript version of this article is solely governed by the terms of such publishing agreement and applicable law.